MONITORING LANDSLIDES USING MULTI-TEMPORAL TERRESTRIAL LIDAR POINT CLOUDS

MWAKA BERNARD
February, 2015

SUPERVISORS:
Dr. Ir. S.J. Oude Elberink
Prof. Dr. Ir. M.G. Vosselman

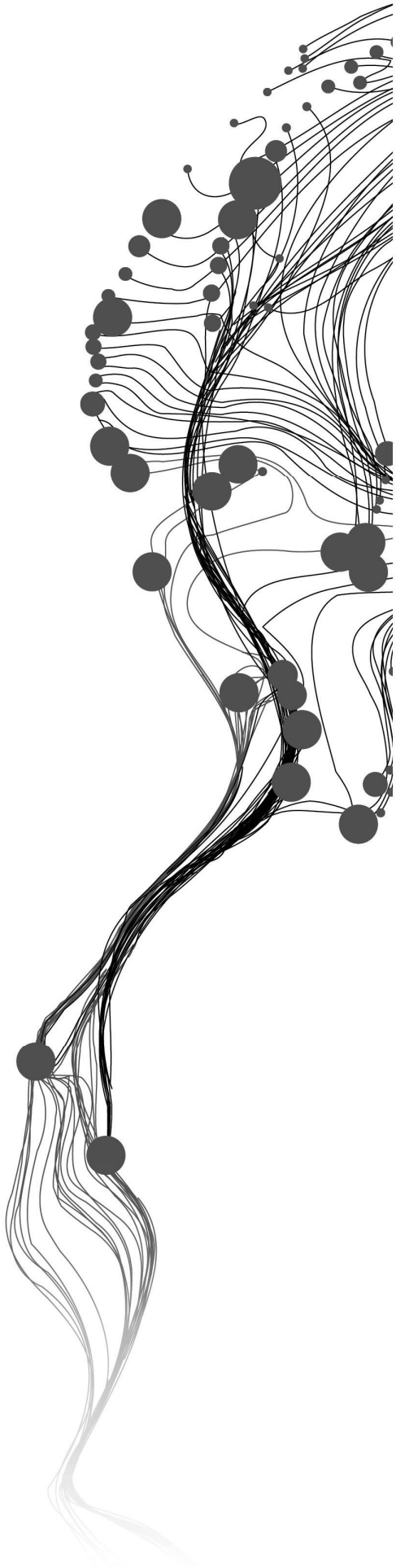

MONITORING LANDSLIDES USING MULTI-TEMPORAL TERRESTRIAL LIDAR POINT CLOUDS

MWAKA BERNARD
Enschede, the Netherlands, February, 2015

Thesis submitted to the Faculty of Geo-Information Science and Earth Observation of the University of Twente in partial fulfilment of the requirements for the degree of Master of Science in Geo-information Science and Earth Observation.
Specialization: Geoinformatics

SUPERVISORS:
Dr. Ir. S.J. Oude Elberink
Prof. Dr. Ir. M.G. Vosselman

THESIS ASSESSMENT BOARD:
Prof. Dr. Ir. A. Stein (Chair)
Dr. M. Rutzinger (External Examiner, University of Innsbruck)

ABSTRACT

Monitoring landslides is of great interest because of the damages they cause to property as well as loss of lives to people. Several remote sensing techniques have been used over the years to monitor landslides. Terrestrial laser scanning is one of such techniques. It offers a promising way to monitor landslides because of its high repeatability and better resolution. The sub objects of a landslide unlike many man-made objects don't have crisp boundaries. Grouping points to objects of a landslide proves to be a challenge as a result. This research presents an object oriented approach that monitors objects in a shallow landslide using multi-temporal terrestrial lidar data. This is achieved by computing the properties of these objects as point attributes in single or multiple epochs. Segment growing, connected components and majority filtering are used to obtain meaningful objects. The height above lowest local point and height difference point attributes are used to separate and group points on trees to single tree segments. Roughness is used to group points on objects of the landslide and low laying vegetation. Post processing using majority filtering led to larger segments to be obtained. The surface separation distance is found to be a useful property of the objects to show change and the size of change.

Key words: shallow landslide, multi-temporal, terrestrial lidar, segmentation, monitoring, surface separation distance

ACKNOWLEDGEMENTS

First and foremost, I would like to thank the Almighty God for his goodness which enabled me to get the opportunity to do my MSc. Degree. But also for the wisdom, knowledge, health and breakthroughs I experienced throughout my study.

I would like to thank and appreciate my supervisors; Dr. Ir. S.J. Oude Elberink and Prof. Dr. Ir. M.G. Vosselman. Thank you for the inspiration and valuable wisdom I obtained working with you in this period. Your support, guidance and encouragement were invaluable.

I would like to appreciate the institute of Institute of Geography, University of Innsbruck for providing the terrestrial lidar data that I used for my research.

To all the staff of the GFM department, thank you so much knowledge I obtained throughout my study. It has surely equipped me for the future.

To all my GFM classmates, you made the journey worthwhile. Thank you all for the encouragement and fun throughout the duration of the course. I would also like to express my thanks to all my colleagues in the other departments.

Lastly, I want to appreciate my entire family for the support and encouragement throughout my study.

TABLE OF CONTENTS

1. INTRODUCTION 1
   1.1. Motivation and problem statement 1
   1.2. Research Identification 2
   1.3. Thesis structure 2
2. LITERATURE REVIEW 3
   2.1. Introduction 3
   2.2. Landslides and its sub-objects 3
   2.3. Lidar in change detection 4
   2.4. Change detection for landslides 5
   2.5. Summary 9
3. METHODOLOGY 10
   3.1. Introduction 10
   3.2. Data pre-processing 11
   3.3. Segmentation 16
   3.4. Object to object matching 20
   3.5. Surface separation distance 21
   3.6. Summary 22
4. RESULTS AND DISCUSSION 23
   4.1. Introduction 23
   4.2. Data sets and study area 23
   4.3. Registration 24
   4.4. Segmentation 27
   4.5. Object to object matching 34
   4.6. Surface separation distance 37
   4.7. Summary 43
5. CONCLUSIONS AND RECOMMENDATIONS 44
   5.1. Conclusions 44
   5.2. Recommendations 45

LIST OF FIGURES

Figure 2-1: Schematic sketch of a shallow landslide 3
Figure 2-2: Schematic sketch of a landslide and labelling of sub-objects of which a shallow landslide is composed of (Cruden and Varnes, 1996) 4
Figure 2-3: Small patches of vegetation or bare land in the landslide eliminated using chessboard segmentation (Martha et al., 2010) 5
Figure 2-4: Final results of landslide identified (a) and the rectangle is for part of the study area in (b)(Deng and Shi, 2014) 7
Figure 2-5: Effects of thresholds on feature extraction (a) and window sizes on curvature calculations (b) (Tarolli et al., 2010) 8
Figure 2-6: Displacement fields calculated for different epochs (Travelletti et al., 2014). 9
Figure 3-1: Framework of the Methodology 10
Figure 3-2: Connected components on points of 2011 epoch. 10
Figure 3-3: Height above lowest local point values for the 2011 large landslide 11
Figure 3-4: Height difference values for 2011 large landslide 12
Figure 3-5: Before using height difference point attribute (a) and (b) after using the height difference point attribute. 13
Figure 3-6: Mean curvature values for 2011 large landslide. 13
Figure 3-7: Roughness values for 2013 large landslide 14
Figure 3-8: Workflow for segmenting points on trees. 16
Figure 3-9: Trees points with height above lowest local point and height difference point attributes calculated 17
Figure 3-10: Working of height difference attribute (a) before and (b) after 17
Figure 3-11: Trees segments after connected components and majority filtering 18
Figure 3-12: Segments on the scarp and landslide boundary with high roughness value 18
Figure 3-13: Workflow showing the segmentation strategy. 19
Figure 3-14: Flow of the matching process 20
Figure 3-15: Workflow showing how the separation distance is computed and used. 21
Figure 4-1: Study area in Schmirntal 23
Figure 4-2: Registration parameters 24
Figure 4-3: Distance between 2011 and 2013 points clouds prior to registration. 25
Figure 4-4: Distance between 2011 and 2013 points clouds after registration. 25
Figure 4-5: Distance between 2011 and 2012 points clouds prior to registration. 26
Figure 4-6: Distance between 2011 and 2012 points clouds after registration. 26
Figure 4-7: Points with values less than 0.5m for the height above lowest local point (a) and (b) are points with values greater than or equal to 0.5m 27
Figure 4-8: points with values for the height difference less than or equal to 1.3m 28
Figure 4-9: Points with height difference values great than 1.3m and height above lowest local point values greater than or equal to 0.5m 29
Figure 4-10: Segment growing results (a) 2011, (b) 2012 and (c) 2013. 30
Figure 4-11: Connected components on points of 2011 large landslide. 31
Figure 4-12: Final segmentation results (a) 2011, (b) 2012 and (C) 2013. 32
Figure 4-13: Scarp area for 2011 (a), 2012 (b) and 2013 (c) data. 33
Figure 4-14: Matching results using minimum distance between 2011 and 2012 epochs. 35
Figure 4-15: Matching result showing several segments matched to one segments 36

Figure 4-16: Surface separation distance between 2011 and 2012 epochs. 37
Figure 4-17: Surface separation distance between 2012 and 2013 epochs. 38
Figure 4-18: Surface separation distance between 2011 and 2013 epochs. 39
Figure 4-19: Segments coloured according to percentage of points that are dynamic between 2011 and 2012 epochs. 40
Figure 4-20: Segments coloured according to percentage of points that are dynamic between 2012 and 2013 epochs. 41
Figure 4-21: Segments coloured according to percentage of points that are dynamic between 2011 and 2013 epochs. 42

LIST OF TABLES

Table 4-1: Transformation parameters for 2012 point cloud.....24
Table 4-2: Transformation parameters for 2013 point cloud.....24
Table 4-3: Colour legend showing colours corresponding to value per point. 38
Table 4-4: Colour legend showing colours corresponding to percentages 41

LIST OF ABBREVIATIONS

2D	Two Dimensional
3D	Three Dimensional
DSM	Digital Surface Model
DTM	Digital Terrain Model

1. INTRODUCTION

1.1. Motivation and problem statement

The use of lidar in the study of gravity controlled flows like landslides is undergoing rapid developments (Ventura et al., 2011; Wang et al., 2013; Tarolli, 2014; Metternicht et al., 2005; Pesci et al., 2011). Airborne lidar has been used to detect historical and active landslides as well as scarps of landslides covered by trees. On the other hand, terrestrial laser scanning has been used to map the foot area of landslides because it achieves better resolution, is portable and has a higher repeatability than airborne lidar (Wang et al., 2013; Abellán et al., 2014)). Because of this, terrestrial laser scanning is mainly used for monitoring purposes and not mapping (Jaboyedoff et al., 2010).

To monitor landslides, several measurements have to be taken at different time periods in order to detect changes. Several remote sensing techniques like satellite imagery, lidar, etc. have been used in literature to monitor these changes.

Methods that use lidar and/ or in combination with other techniques have been reported by some authors (Anders et al., 2013; Dewitte et al., 2008; Razak et al., 2013). These methods make use of DTM's extracted from lidar at different time stamps and subtract these DTM's for a specific geomorphological activity; changes are then interpreted from the results. The approaches that use DTM's/ DSM's to perform volume computations as an indicator of change don't explicitly demonstrate which objects within the landslides changed i.e. they depict a general impression of change. In addition, approaches that use DTM's only the 2.5D structure of the scene is analysed instead of 3D structure which is offered by object based methods that use 3D point clouds (Rottensteiner, 2010).

Image based techniques that group pixels into objects based on some homogeneity criterion have been researched and developed in (Lu et al., 2011; Van Den Eeckhaut et al., 2012). These methods extract features from imagery and classify them into classes based on some rules. Volume changes per category are computed to detect changes. Other methods detect changes by grouping pixels into change classes i.e. stable, positive and negative (Hervás et al., 2003). Pixel based methods have the disadvantage that for places with mixed pixels, the centre pixel is an average/ aggregation of different DN values which could belong to different objects. In essence the information about objects is lost and the pixel value is not a true reflection of all objects within that pixel; this affects accuracy of the change detection. This is also the case with methods that use DTM which are also pixel based.

However, there is still no technique that monitors objects within a landslide using lidar point clouds. Whereas a lot of work has focused on the detection and extraction of man-made objects like roads, buildings (Teo & Shih, 2013) and trees (Xiao et al., 2012) from point clouds, not much has been done for natural processes like landslides. Unlike man-made objects which have crisp boundaries and defined geometries, natural objects don't have these properties. The challenge is then how to group points in a point cloud as landslide objects and monitoring how these segments/ objects change over time. In light of the limitations given by previous methods and the advantage that object based analysis offers, this study is motivated towards monitoring landslides by looking at objects/ segments in the point clouds to detect changes. The aim is to have a one to one relation between segments in order to link objects of interest

1.2. Research Identification

1.2.1. Research objectives and questions

The main objective of the proposed research is to develop an object oriented approach that detects changes of a shallow landslide in 3D multi-temporal terrestrial laser scanning point clouds.
The main objective will be achieved through the following sub-objectives;

1) To determine the characteristics of objects of a landslide.
    - What are the important properties of landslide objects?
    - What properties of landslide objects can be derived in a single epoch of a terrestrial laser scanning dataset?
    - What properties of landslide objects can be derived in multiple epochs of terrestrial laser scanning datasets?
2) To group points of 3D terrestrial laser point cloud to objects of a landslide.
    - What is the optimal segmentation strategy to group objects?
    - How sensitive is the segmentation to noise?
3) To detect changes at object level in TLS point clouds.
    - How to match corresponding objects in the two epochs?
    - What properties of these objects can be used to measure change?
4) To perform quality assessment.
    - What is the quality of the segmentation?
    - What is the quality of the matching?

1.2.2. Innovation aimed at

The innovation in this research will be an approach that employs object based analysis to detect changes in landslide using 3D terrestrial laser scanning point clouds. This will be accomplished by segmenting the point clouds and monitoring what happens with the segments over time.

1.3. Thesis structure

The thesis is organised into six chapters. The first chapter is the introduction that contains the motivation and problem statement, research objectives and questions and innovation aimed at in this research. The second chapter covers the literature review on landslides, lidar in change detection and change detection for landslides. The third chapter describes the methodology that was used for this research. Chapter four presents the results and a discussion of the results. Chapter five describes the conclusions and recommendations for future research.

2. LITERATURE REVIEW

2.1. Introduction

In this chapter, a review is made on landslides and its different sub objects in section 2.2. The use of lidar in change detection is discussed in section 2.3 and then finally change detection for landslides is discussed in section 2.4.

2.2. Landslides and its sub-objects

Natural disasters such as earthquakes, tsunamis, floods, landslides and volcanic eruptions pose a threat to lives and property but also inflict heavy economic losses. Of these, landslides are especially more pronounced in mountainous regions. They are triggered by human activities, heavy rain fall and earthquakes (Chung et al., 2014). According to figures released by Center for Research on the Epidemilogy of Disasters (2012), landslides accounted for 7.5% of the total reported deaths and 11.8% of total damages caused by natural disasters.

Landslides can be defined as downward and outward displacement of materials that are induced by gravity (Gutiérrez et al., 2010). Several types of landslides exist and these are classified based on movement mechanism, nature of slope material, form of rupture surface and rate of movement (Goudie, 2004). Martha et al. (2010) and Cruden and Varnes (1996) classified landslides based on the type of movement as falls, topples, rotational slides, translational slides, lateral spread, flows and complex. Regmi et al. (2013) further grouped landslides into shallow and deep seated landslides. In this study the focus is on shallow landslides (Figure 2-1), which are characterized by a maximum depth of 2m and it's composed of debris slides, debris flow and soil slides. These shallow landslides are located in the Alpines slopes and are often caused by melting of snow and heavy rainfall (Wiegand et al., 2013).

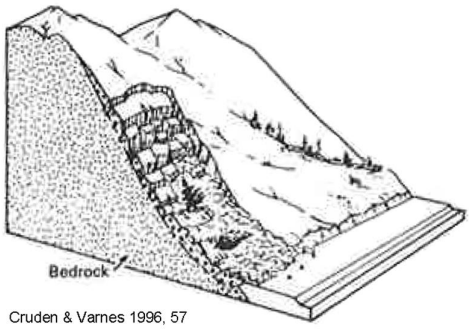

Figure 2-1: Schematic sketch of a shallow landslide(Cruden & Varnes, 1996)

A landslide consists of several sub objects (Figure 2-2) that can be distinguished from another using various properties.

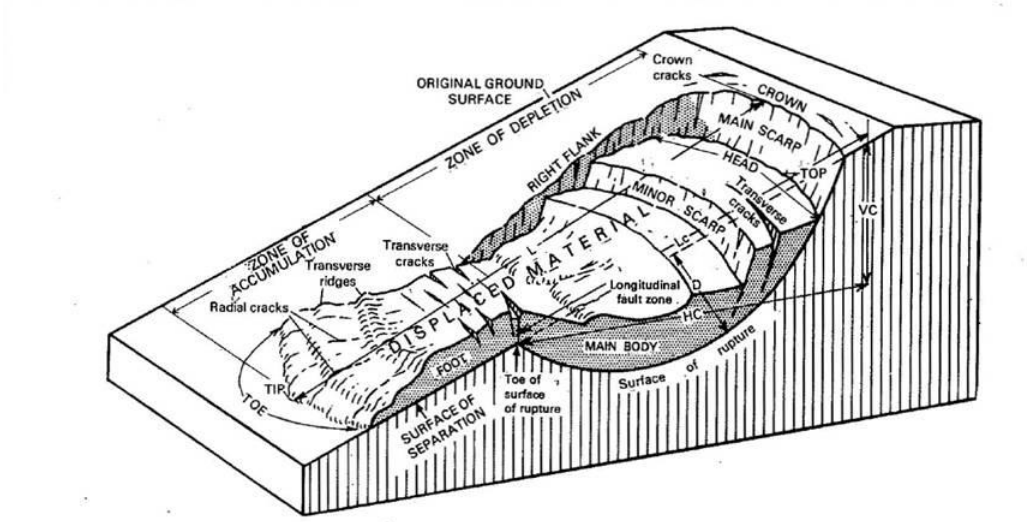

Figure 2-2: Schematic sketch of a landslide and labelling of sub-objects of which a shallow landslide is composed of (Cruden and Varnes, 1996).

2.3. Lidar in change detection

The use of light detection and ranging (lidar) for change detection in many application fields is becoming more and more prominent. This is because of its capacity to acquire 3D information accurately and hence changes can be visualized in three dimensions. Several studies have used lidar for change detection.

Choi et al. (2009) proposed a feature based change detection method for urban areas that uses two different lidar epochs. A height difference image from the digital surface models generated from lidar is computed from which segmentation and classification of the surface patches was performed to detect changes. Xu et al. (2013) detected changes in building using multi-temporal airborne laser scanner data. Surface separation was used to distinguish between changed, unchanged and unknown parts of buildings. This separation value was calculated as the distance a point and a plane fitted through the neighbours of its nearest point in the other epoch. The points of the buildings that changed were further classified using attributes like normal of the nearest roof, area and height to the nearest roof. Their approach correctly detected 80% of building changes. Vögtle and Steinle (2004) demonstrated the use of height difference for segmentation of laser scanner derived normalised DSM's. With their approach nearly all buildings were segmented but vegetation points were not because they didn't satisfy the set tolerance. The height difference was then used to detect changes. Murakami et al. (1999) also used DSM's derived from airborne laser scanner for change detection. The authors used a difference image to detect changes in the buildings. This difference image was generated by subtracting the DSM's from each other.

Xiao et al. (2012) used multi-temporal airborne lidar point clouds to detect changes in trees in urban areas. The authors applied connected component algorithm to group point of trees together and then used the attribute of the component to distinguish vegetation from other features like buildings. 3D alpha shapes, convex hull and 3D tree modelling are used to derive the tree parameters. A point based tree to tree matching algorithm that utilizes overlapping bounding boxes and point to point distances is used to match the trees in the different datasets. Change is detected by comparing the volume and area of each tree component. Teo and Shih (2013) used multi-temporal interpolated lidar data for change detection and change type determination using geometric analysis. A height difference map was utilized to locate potential areas of change.

2.4. Change detection for landslides

Numerous studies have reported the use of images for change detection of landslides. Roessner et al. (2014) employed multi-temporal satellite imagery to automatically detect changes in landslides using trajectories of NDVI values derived from the images. Hervás et al. (2003) on the other hand used multi-temporal orthoimages to detect changes in a landslide. They proposed a method that is based on image differencing and subsequent thresholding into change classes i.e. stable, positive and negative. The positive and negative classes represent areas of change while the stable class shows areas that didn't change.

Lu et al. (2011) detected changes in a landslide using very high resolution optical images. They used scale optimization to segment the image and then applied spectral and textural metrics for multi-temporal analysis of the landslide objects. Martha et al. (2010) identified objects in a landslide by first segmenting the image using the multi-resolution segmentation algorithm. Post processing to resegment mixed segments was done using chessboard segmentation technique and false positives eliminated using NDVI values as a threshold. Classification of the extracted objects was done using expert knowledge. Their approach detected 76.4% of five landslide types with 69.1 % classification accuracy. Qiao et al. (2013) also used the NDVI value but in addition defined a vegetation damage index. This value was computed as the difference between NDVI values obtained from the pre and post landslide activity images. This vegetation damage index value is then used to recognise the landslides.

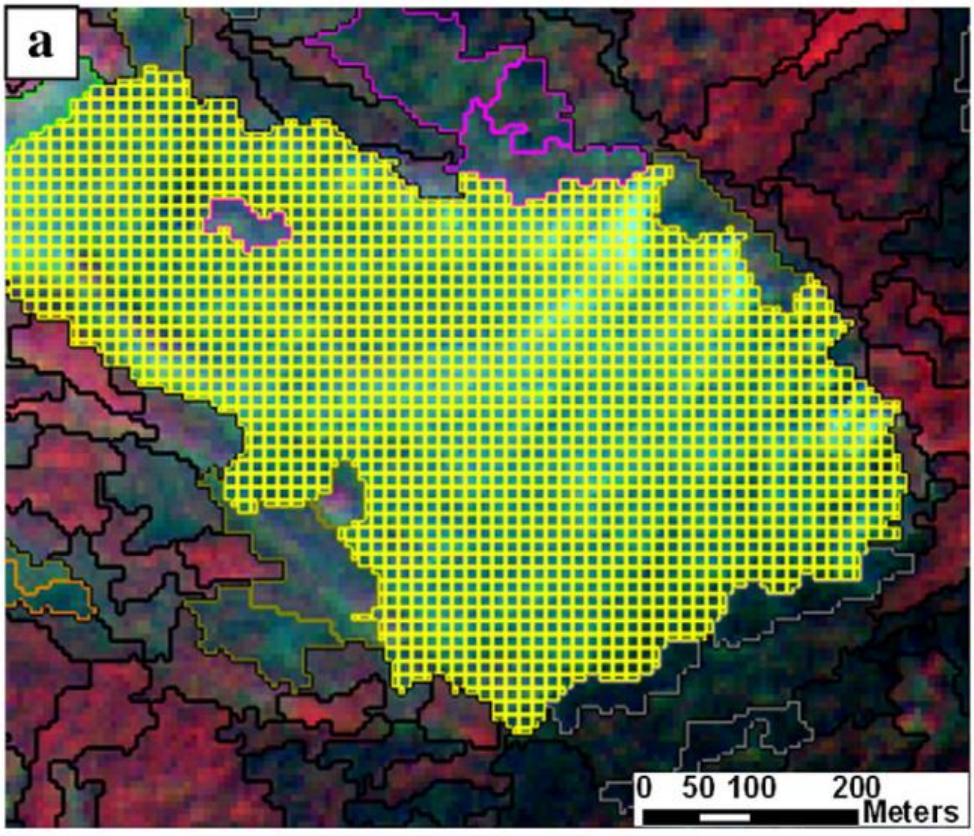

Figure 2-3: Small patches of vegetation or bare land in the landslide eliminated using chessboard segmentation (Martha et al., 2010)

Automatic reconstruction techniques for landslides from optical images have also been researched on. Stumpf et al. (2015) monitored erosion and deformation on a landslide using Structure-from-Motion and Multi-View Stereo techniques. Point clouds from the images of the landslide were created through dense image matching and then registered using the Iterative Closest Point algorithm. In order to assess the accuracy of the derived point clouds, a Multi scale Model to Model Cloud computation (M3C2 algorithm) was used to compare the point clouds with terrestrial laser scanning and airborne laser scanning scans. Changes were using the M3C2 algorithm by looking at the distance between the point clouds. However, this approach is limited for monitoring landslides covered with vegetation since the passive optical sensors cannot penetrate through the vegetation. It is also less precise as compared to the use of terrestrial laser scanning data.

Several studies have made use of lidar alone or in combination with other techniques. Ventura et al. (2011) monitored an active landslide in Italy using lidar derived digital terrain models acquired on different dates. Interpretation and statistical analysis of variations of surface roughness and residual topographic surface were utilized to reconstruct and track the landslide. Anders et al. (2013) in addition incorporated the use of stratified feature extraction algorithm to semi-automatically extract features. Volume change for each extracted object is used as a basis for detecting changes in the landslide. Van Den Eeckhaut et al. (2012) identified objects in a forested landslide using single pulse lidar derivatives like slope gradient, roughness, openness and curvature. Thresholding and multi-resolution segmentation are applied to extract features after which support vector machines are used for classification. Dewitte et al. (2008) used multi-temporal DTM's derived from aerial stereo photogrammetry and airborne lidar data to measure landslide displacements. The difference between the DTM's was used as an indicator of the horizontal and vertical movements of the landslide. With their approach they were able to identify displacements at the main scarp and within the landslide.

Glenn et al. (2006) used surface roughness, slope, semi variance and fractal dimension derived from airborne lidar data to characterize and differentiate morphological components of a landslide. Surface roughness and fractal dimension were noted to be greater at the toe than at the body or upper block of the landslide. Their work also showed that high resolution topographic information can aid in the analysis of landslide activity and material type. However, the use of fractal dimension and semi variance to describe topographic variability is limited to the scale and the location of the area of interest. McKean and Roering (2004) used high resolution DEMs from airborne lidar data to characterize a landslide. In order to map roughness from the DEMs, one dimensional, two dimensional (circular) and three dimensional (spherical) statistics were used. The value of roughness was measured in sampling windows and was used to separate the landslide from adjacent stable areas. Kinematic units within the landslides were correctly delineated using local variability of aspect. However, the selection of the sampling window size and grid resolution is rather subjective. Similarly, Razak et al. (2011) proposed a method that maps and identifies morphological features of landslides using DTMs derived from airborne laser scanning data. However, they also included the use of filters for mapping the landslide i.e. one filter from progressive TIN densification and two filters from hierarchical robust interpolation. The landslide filter based on hierarchical robust interpolation is used because of the advantage it offers when dealing with complex terrain especially one that is forested. Their work demonstrates that the landslide filter yields the best outputs with errors for the scarps and cracks lower when no vegetation is present. On the other hand, the errors are fairly similar for both the forested and open terrain for the rock blocks. Consequently, the DTM derived from airborne laser scanner data shows a vast improvement in landslide recognition and classification in comparison with optical images. Although the use of a single DTM to assess a dynamic phenomenon like a landslide is not optimal. Tarolli et al. (2010) proposed a method to automatically detect crowns and bank erosion of a shallow landslide. Their approach used thresholds obtained from statistical analysis of curvature to detect these geomorphic features. Figure 2-5(a) shows the effects on selecting threshold values 1, 2, 3 and 4 on feature extraction. The authors also tested the effect of moving window size on curvature calculation as

shown in Figure 2-5(b). It was noted that small window sizes were not good since they took into consideration only a limited area. Very large windows were also found not to be optimal. Therefore, the window size should be related to the size of the features that will be extracted. A threshold value of 1.5 of the inter quartile range and a 21 x 21 moving window size yielded the best results for feature extraction. In addition, their work showed that the use of thresholds was efficient for the extraction of features. However this method is not suitable for areas with complex morphologies. Deng and Shi (2014) employed airborne lidar data to semi-automatically detect landslides. Landslide components are first extracted by identifying morphological features related to them and then the landslide is separated from other terrain objects using geometric and contextual analysis. 93.5% of recent and 23.8% of old landslides were extracted through this approach. Morphological features like the main scarp and rupture floor were identified using statistical significance tests. However, the thresholds used in their work are arbitrary and limited to the study area. Similarly, Chigira et al. (2004) also detected new and old landslides using airborne lidar data. In addition they made use of aerial photo graphs and geological based ground truth to investigate the landslides. Unlike the aerial photographs, the laser scanner map they created was able to show both previous and current landslides.

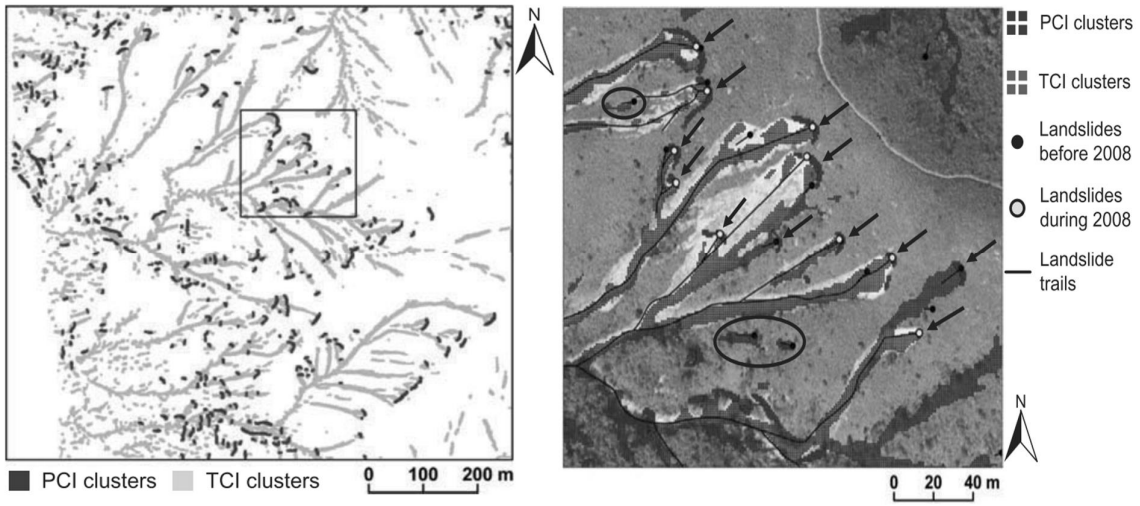

(a) (b)

Figure 2-4: Final results of landslide identified (a) and the rectangle is for part of the study area in (b)(Deng and Shi, 2014)

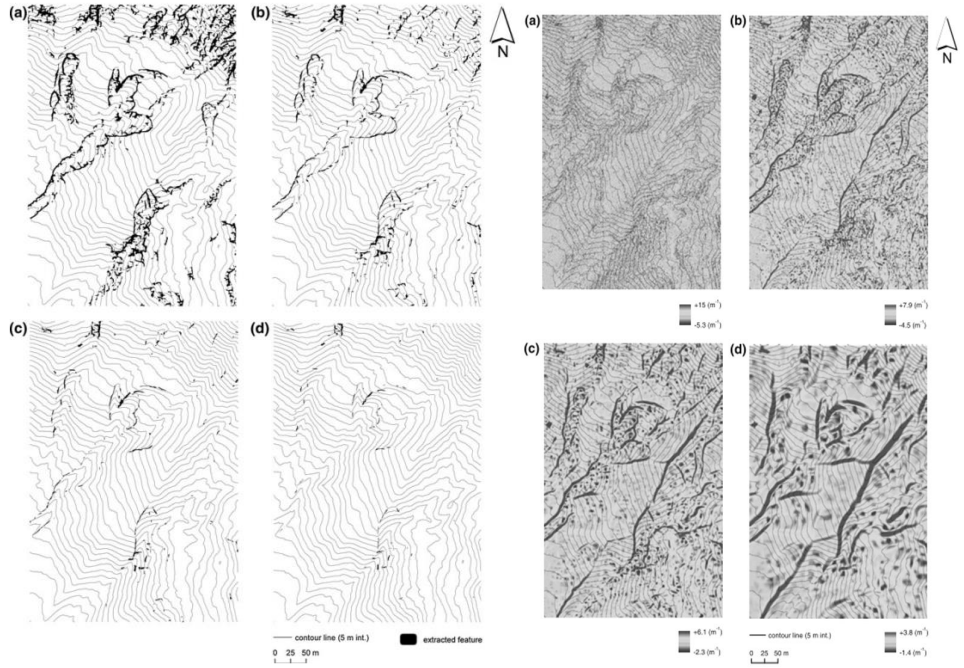

(b) (b)

Figure 2-5: Effects of thresholds on feature extraction (a) and window sizes on curvature calculations (b) (Tarolli et al., 2010)

Travelletti et al. (2014) used an image based correlation on multi-temporal terrestrial laser scanning point clouds to measure 3D displacements fields and deformation of a landslide. The displacement field was first calculated in 2D using a normalized 2D cross correlation function. The calculated 2D displacements were the reconstructed to 3D by using a bilinear interpolation which linked the X, Y, Z coordinates in the point clouds to the displacement vectors in the images. A median filter was used to remove outliers from the displacements and thereafter strain fields were calculated to show the deformation patterns. Their approach showed that the use of displacement fields provided more insight on the movement of landslides. The bilinear interpolation used in their work reduces shadow effects on displacement field calculations. However, the 2D correlation function used in their work cannot handle distortions related to the use of perspective projection.

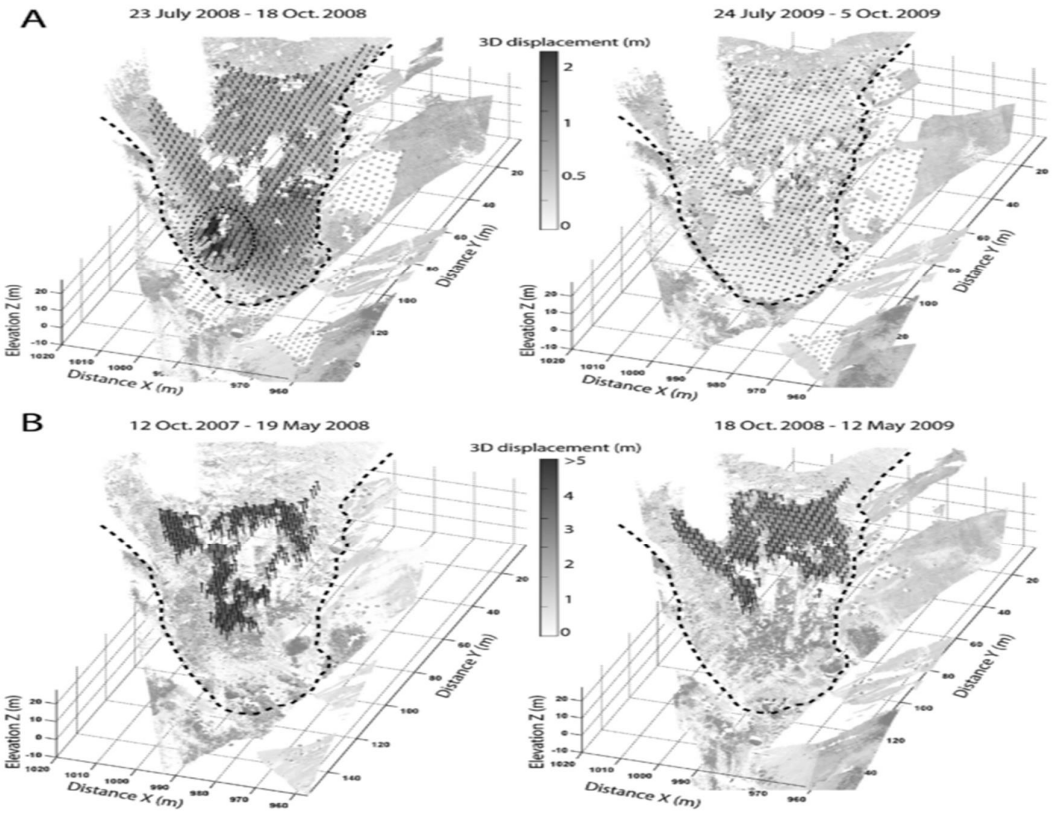

Figure 2-6: Displacement fields calculated for different epochs (Travelletti et al., 2014).

2.5. Summary

Remote sensing is a powerful tool in the study of landslides. Several techniques like lidar and the use of images have been applied to this effect. Whereas a lot of literature on the use of images in object based change detection has been done, these techniques are limited because the pixel values that are grouped into segments don't wholly represent all objects that fall within one grid cell. As a result, information about some objects is lost. Moreover these techniques only describe changes in 2D. Research has been done on the use of lidar in change detection predominantly uses DTM's/ DEM's to show changes. Because of this, we propose methods that group points in lidar point clouds to objects of a landslide. These methods make sure of the properties of these objects.

3. METHODOLOGY

3.1. Introduction

In this chapter, we describe the methodology that was followed to answer the questions of this research. Section 3.2 describes the pre-processing that was done on the data and also the computation of point attributes. Section 3.3 describes how the segmentation process was done. Section 3.4 describes the matching process. Section 3.5 describes how the surface separation distance was computed.

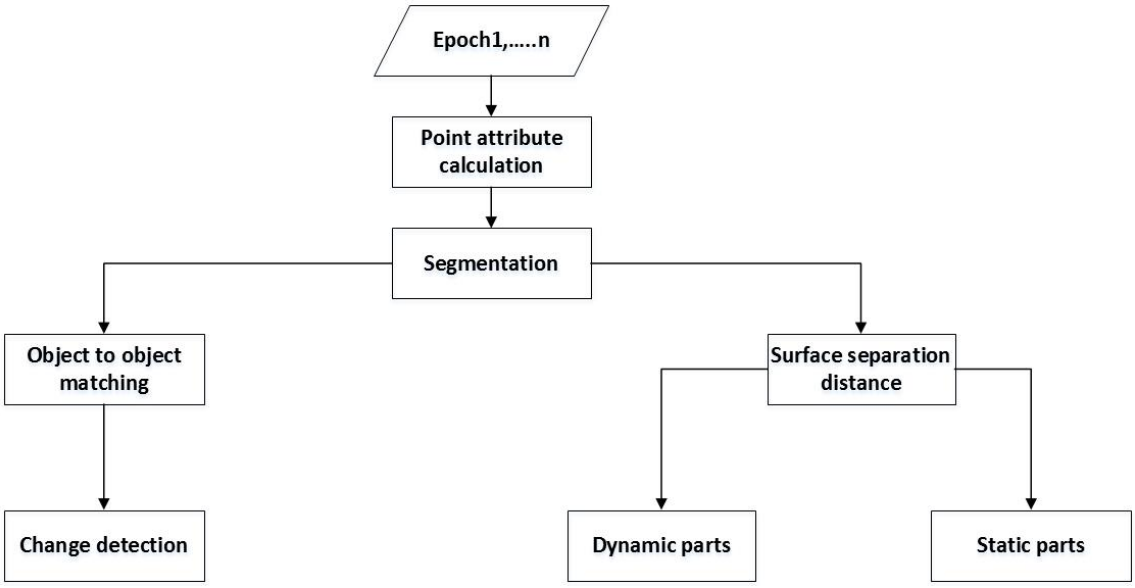

Figure 3-1: Framework of the Methodology

The frame work of the methodology as shown in Figure 3-1 was adopted because when a segmentation based on connected components was tested on the datasets, it didn't yield a good output as shown in Figure 3-2. Most of the points were grouped into one large segment. As a result, we followed the methodology framework shown in Figure 3-1 that takes into consideration the properties of the objects of the landslide. These properties are computed as point feature values and are used to group points to objects and thereafter monitor if these objects change or not. Two methods i.e. object to object matching and the use of the surface separation distance were tested for monitoring of the objects. Object to object matching was used because it makes use of the object properties while the surface separation distance makes use of the multi-temporal epochs.

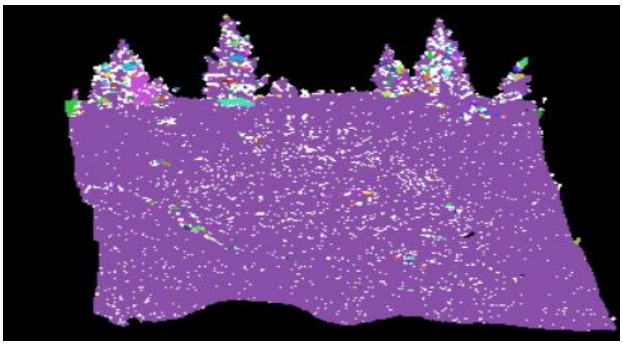

Figure 3-2: Connected components on points of 2011 epoch.

3.2. Data pre-processing

It is often assumed that point clouds are usually correctly registered but this might not be the case so it's good to check the point clouds before any processing is made on them. Landslides are geomorphologically complex and such consist of different sub objects with different characteristics (Van Den Eeckhaut et al., 2012). With this knowledge, we identified the characteristics of these sub objects that were present in the study area. The identification of appropriate characteristics is important because it has a bearing on the success of the extraction of the sub objects. These characteristics were calculated as point attributes in the point clouds with the idea that they could be used to distinguish the different sub objects. These included; slope, curvature, roughness, separation distance between two epochs, height above lowest local point and the height difference between the maximum and minimum Z value within a local neighbourhood. The height above lowest local point and the height difference point attributes were computed using a 2D neighbourhood of 120 points with a radius of 0.3m. The rest of the attributes were computed using a 3D neighbourhood of the same number of points and radius. Using a neighbourhood of 120 points means that the attribute calculation per point will be influenced by its nearest 120 neighbours. Curvature however was computed using CloudCompare software. The rest of the attributes were calculated using C++ programming language.

3.2.1. Height above lowest local point

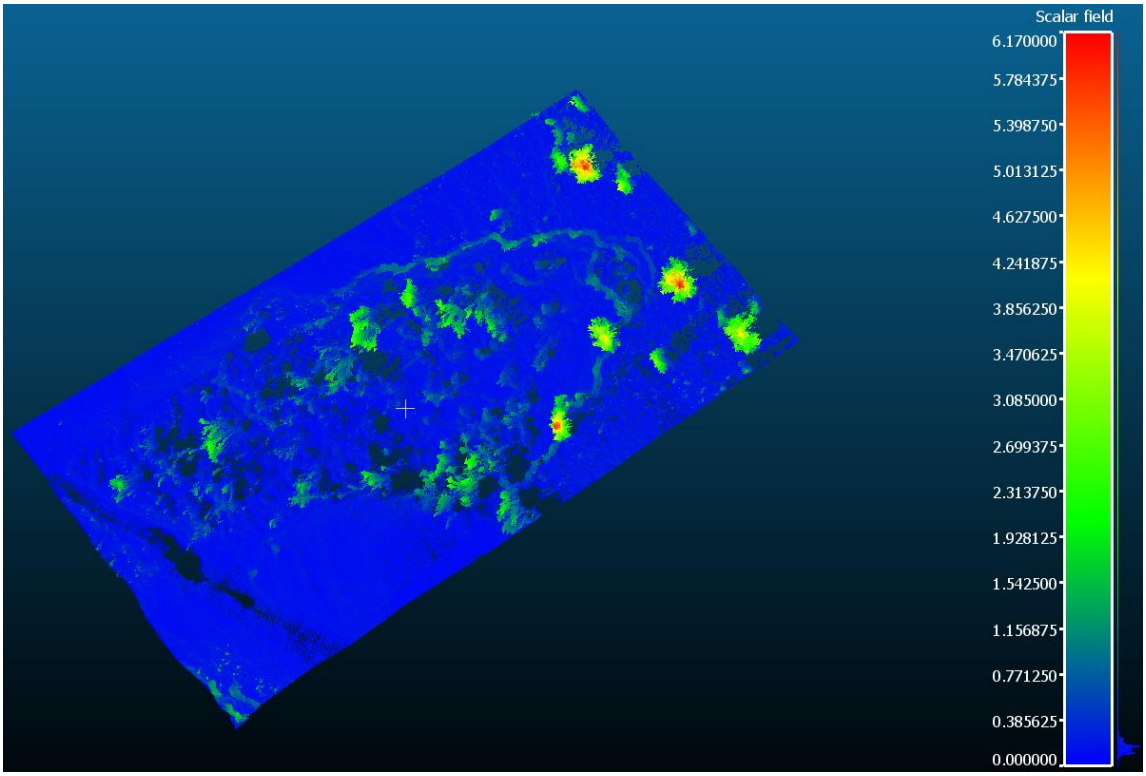

Figure 3-3: Height above lowest local point values for the 2011 large landslide

Figure 3-3 shows values of the height above lowest local point calculated for the 2011 large landslide. The values varied from 0 to 6.17m. Large values were observed on trees and some low laying vegetation present in the data. The terrain was observed to have small the smallest values. The large values for the points on trees and some low laying vegetation was because in a 2D neighbourhood, the lowest point will most likely be at the bottom of the tree. Therefore, the difference between the Z value of any point and

height of the lowest local point will be lager as you go to the top of the tree. This is not the case for points on the terrain where the difference between the Z of any point and the lowest local in a 2D neighbourhood will be small since the points are in close proximity. This attribute was later used to eliminate points on trees from the dataset. In order to retain points on the terrain (which include the points on the sub objects of the landslide), this point attribute was used in combination with the height difference attribute to keep apart points on trees and low laying vegetation. This attributed was calculated as the difference between the Z value of a point and the lowest height value in a local 2D neighbourhood consisting of 120 points.

3.2.2. Height difference

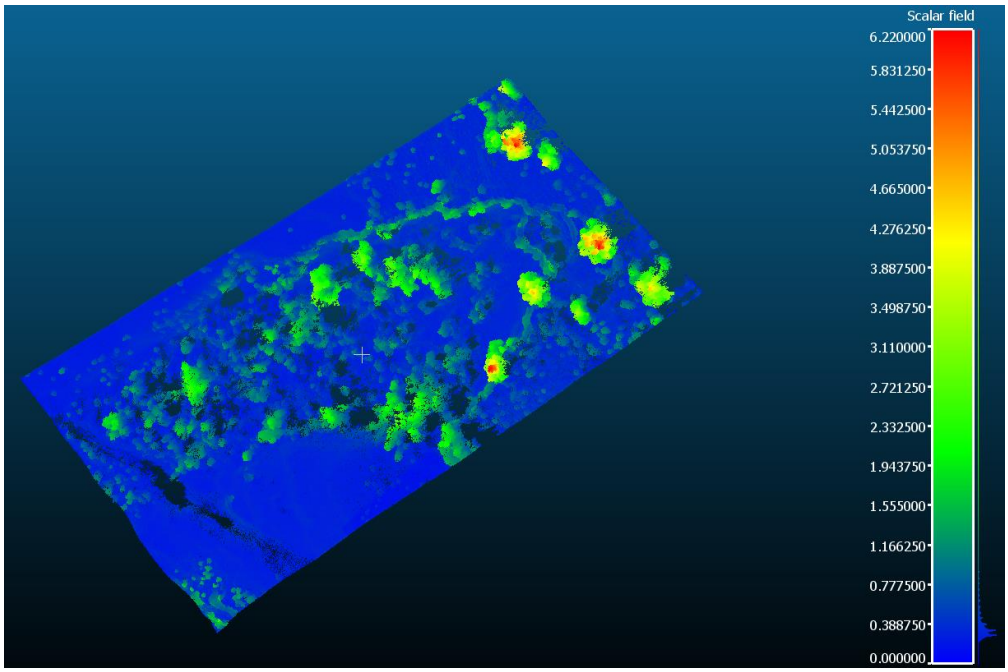

Figure 3-4: Height difference values for 2011 large landslide

Large height difference values were observed mostly on trees and some low laying vegetation as shown in Figure 3-4. This was as expected because the difference between the highest and lowest height values for points on trees and low laying vegetation is always large. For the points on the terrain, low height difference values were observed. This is because the terrain is largely flat so in a local neighbourhood, the height difference values are expected to be small. This attribute was used to in combination with the height above lowest point attribute to further separate terrain points that have high values of the height above lowest point attribute as shown by the grey circle in Figure 3-5 (a). These terrain points however have lower values of the height difference point attribute than trees and low laying vegetation. These terrain points are separated from the points on the tree by using the height difference point attribute (Figure 3-5 (b)). This point attribute was calculated as the difference between the maximum and minimum Z value in a local 2D neighbourhood of 120 points. This point attribute was used to separate points on the tree from points on the terrain.

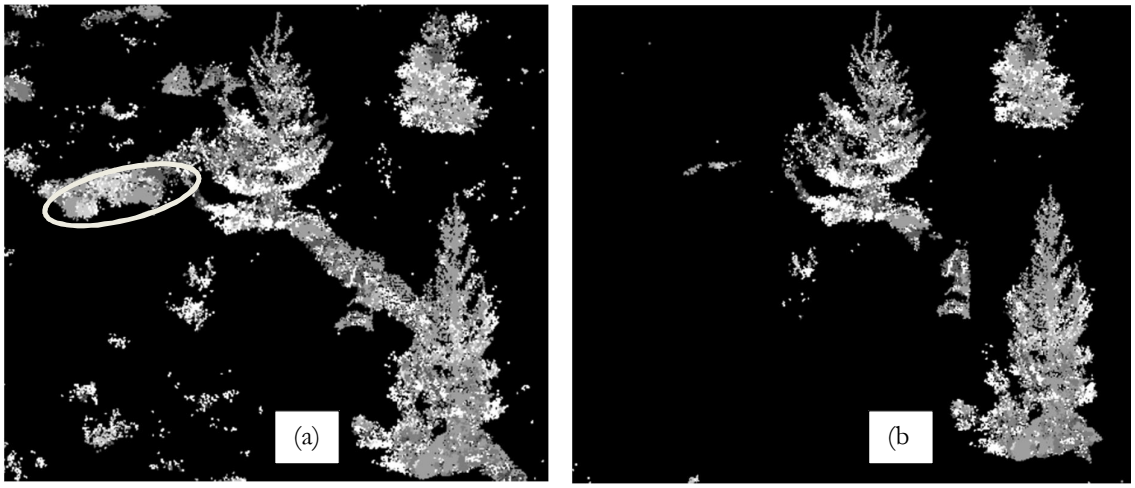

Figure 3-5: Before using height difference point attribute (a) and (b) after using the height difference point attribute.

3.2.3. Mean curvature

In this study we used the curvature because it is a property that can be used to discriminate the scarp from the rest of the objects in the dataset. This is because the shape of the scarp means it will have high values for the curvature as compare to any other object.

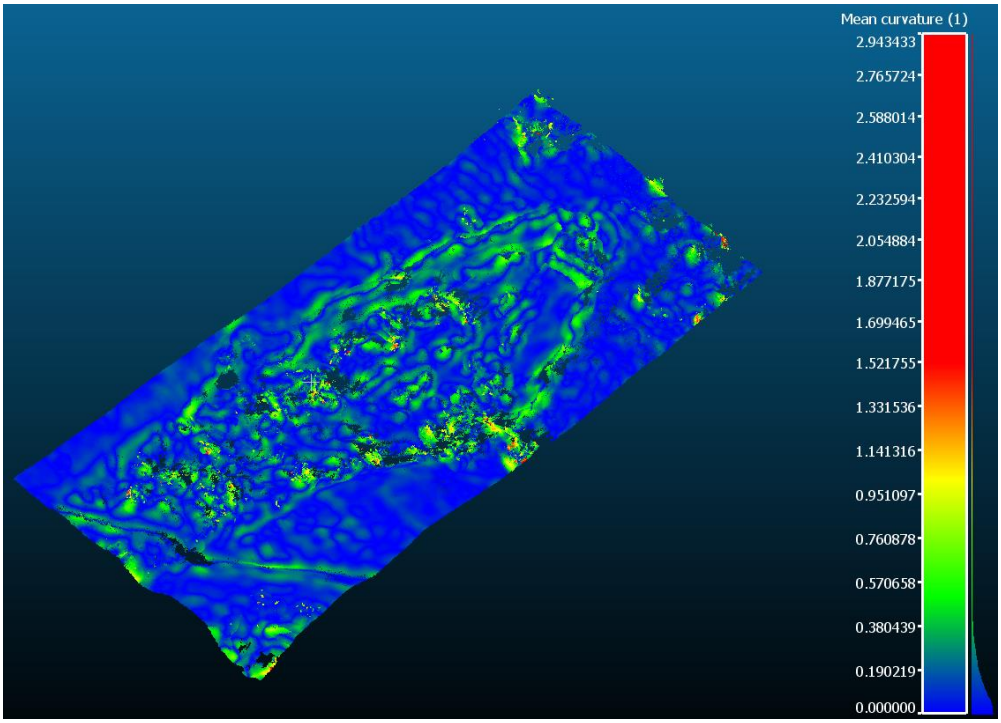

Figure 3-6: Mean curvature values for 2011 large landslide.

The values of curvature were computed at a radius of 1m using CloudCompare as shown in Figure 3-6. It was observed that the highest values were not necessarily on the scarp as expected but on other points on the terrain (red colour). The points on the scarp, boundaries of the landslide and some parts of the landslide had lower values as indicated by the green colour in Figure 3-6. This is likely due to the radius that was used in computing this point attribute. Probably a radius that approximates the radius of the scarp would be suitable since the curvature is a global value. But then again computational wise, its more tasking the longer the radius used to select points that are used in calculating this point attribute.

3.2.4. Slope.

The slope is a property that is characteristic of the scarp and flanks of the landslide. This is because they have steep slopes as compared to the rest of the sub objects of the landslide (Van Den Eeckhaut et al., 2012). Van Den Eeckhaut et al. (2012) used thresholding on slope to extract the scarp. With a high threshold value they were able to extract the scarp. This point attribute in combination with the curvature would be good to group points on the scarp together after the trees and low laying vegetation have been separated from the terrain.

The slope was computed as follows:

- Slope = acos (fabs(normal.Z()))

3.2.5. Roughness

Roughness was calculated in a 3D neighbourhood consisting of 120 points. The choice of using a 3D neighbourhood is because since this attribute is a local value calculating values per point would mean using a few points around a particular point. This gives an accurate representation of this attribute value. With a 2D neighbourhood more points will be considered in point attribute calculation leading to low values since the influence of many points will introduce noise in point attribute calculation.

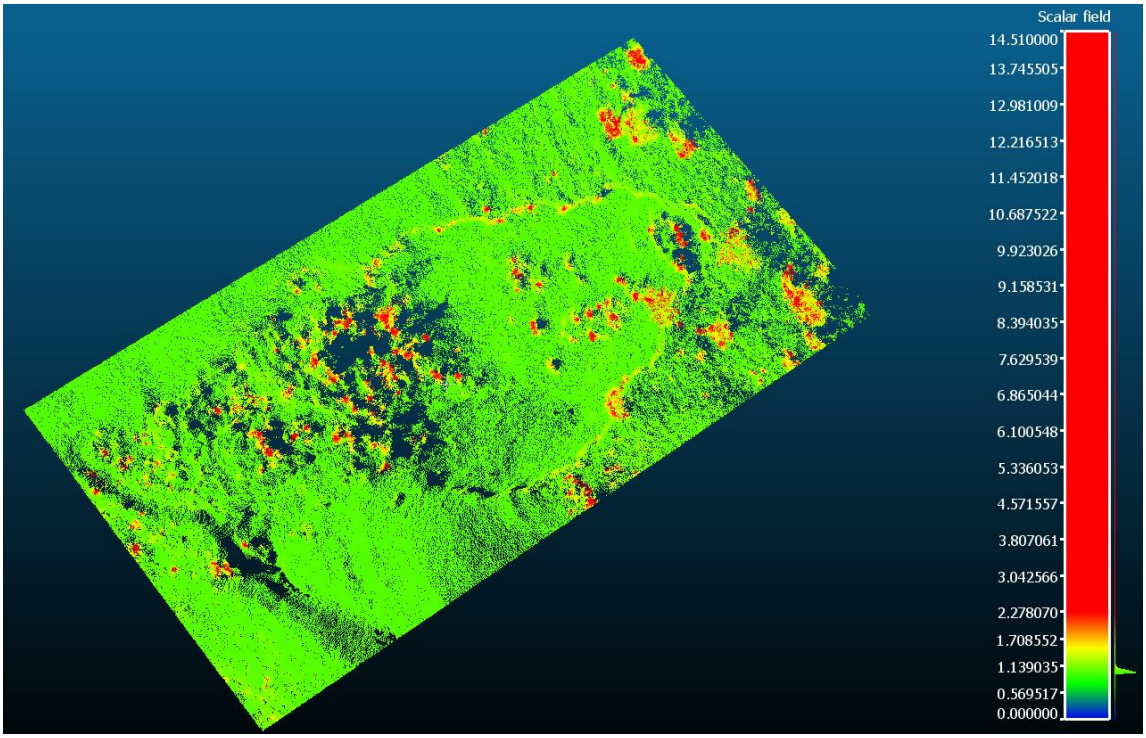

Figure 3-7: Roughness values for 2013 large landslide.

High values for roughness were observed on points of trees and low laying vegetation. Points on the terrain had low values. This point attribute was later used an attribute in the segmentation process.

- Roughness = (eigen [2] + eigen [0]) / (eigen [2] - eigen [0]).

Roughness was defined as the inverse of flatness where the eigen values correspond to the eigen vector which describes the normal of the surface.

3.2.6. Surface separation distance.

In order to make use of the point clouds of the study area captured in different years, the surface separation distance was used. It is a property of the sub objects of the landslide that can be computed between multi-point clouds. This point attribute was used after the segmentation process to indicate which segments were changing and by how much they were changing. This attribute was computed for each point by looking for its nearest neighbour in the other epoch and then fitting a plane through its nearest 20 neighbours. Perpendicular distances to this plane were then calculated. This attribute was later used to differentiate between segments that are static and those that are dynamic.

3.3. Segmentation

In order to detect objects, segmentation was performed on the points to group them into segments that belong to objects. Segment growing, connected components and majority filtering algorithms were used. In this study we used the segment growing segmentation method because the study area contains a large number of points that belong to non-planar objects. Segment growing algorithm is particularly suitable for non-planar segments (Vosselman, 2013). The connected components algorithm is good for grouping points close by belonging to a segment. Neighbouring points are only added to a segment if they are within a given distance threshold. Xiao et al. (2012) used the connected components algorithm to group points on trees and to separate vegetation from non-vegetation point. Majority filtering algorithm assigns unsegmented points to the most frequent segment number within a defined neighbourhood radius. Vosselman (2013) used this filter to obtain larger segments on vegetation.

3.3.1. Separation of points on trees

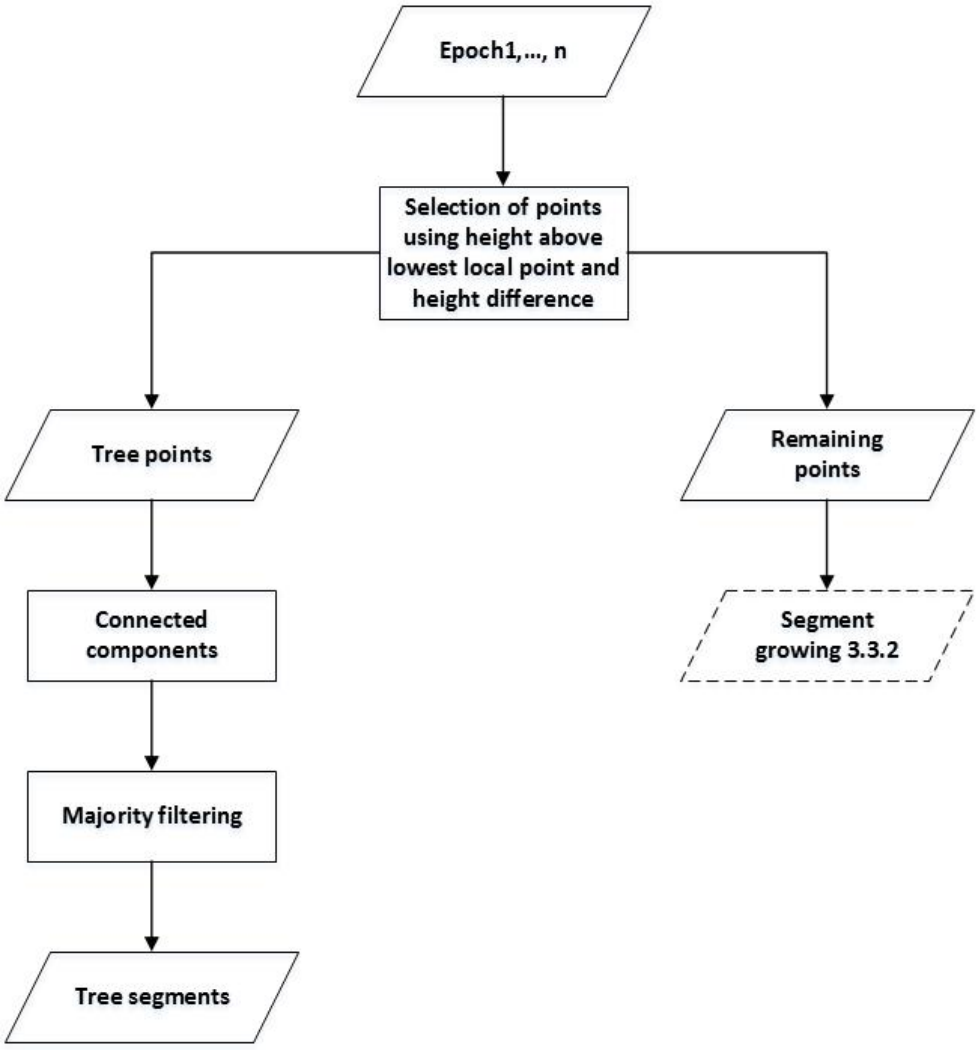

Figure 3-8: Workflow for segmenting points on trees.

In order to separate points on trees from the rest of the points, point attributes of height difference and height above lowest local point were used. The height above lowest local point was used as an attribute because points on trees and low laying vegetation will typically have large values than points on the terrain.

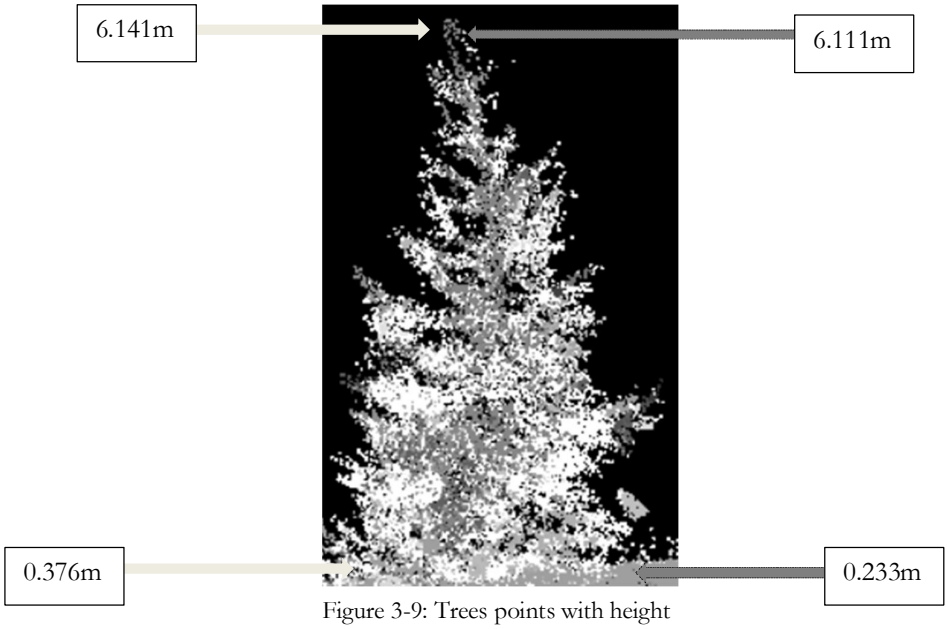

Figure 3-9: Trees points with height above lowest local point and height difference point attributes calculated.

The height difference attribute was used to further separate points on the terrain, low laying vegetation and trees that were still mixed after making a selection based on the height above lowest local point. Similarly, points on trees and low laying vegetation will have higher values than points on the terrain for this attribute. Figure 3-9 shows the working of these two point attributes. The grey arrows show values for the height difference attribute on top of the tree and on the terrain. The dark grey arrows show values on top of a tree and on the terrain for the height above lowest local point. This difference in value shows that with a threshold we can separate the points on the tree from the terrain. A selection was made on points with values for the height above lowest local point attribute greater than a given threshold value. Points below this value were kept away. These points belonged to the terrain. To further separate the remaining terrain points from points on trees and low laying vegetation, a selection was made on points with a given height difference value. This separated the terrain points from points on trees and low laying vegetation.

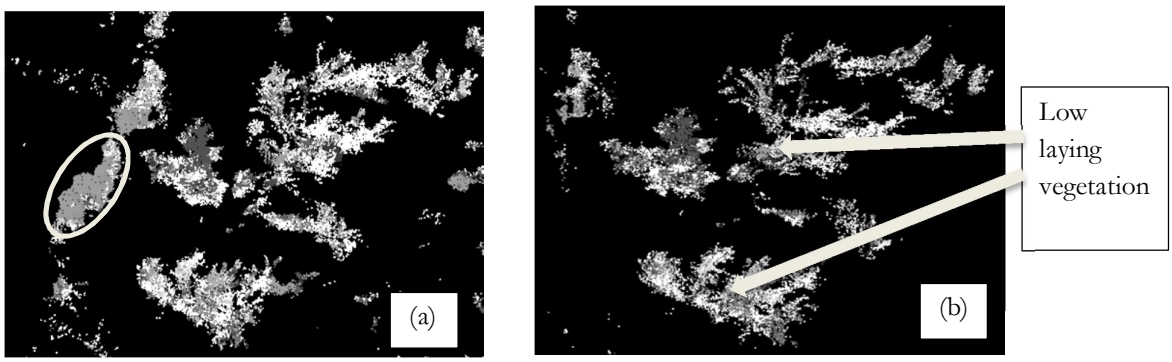

Figure 3-10: Working of height difference attribute (a) before and (b) after

Figure 3-10 shows how the height difference attribute separates points on terrain from low laying vegetation. The grey circle in Figure 3-10 (a) shows the terrain points that were still present after using the height above lowest local point attribute. After using the height difference attribute these points were removed as shown in Figure 3-10 (b). This output was then combined with the terrain points previously kept to form an output of points on the terrain. The remaining point set containing points on trees and low laying vegetation were grouped into segments using a connected components analysis. Majority filtering was then applied to assign non-segmented points to segments that were nearby within some radius. The output was segments on trees and some low laying vegetation as shown in Figure 3-11.

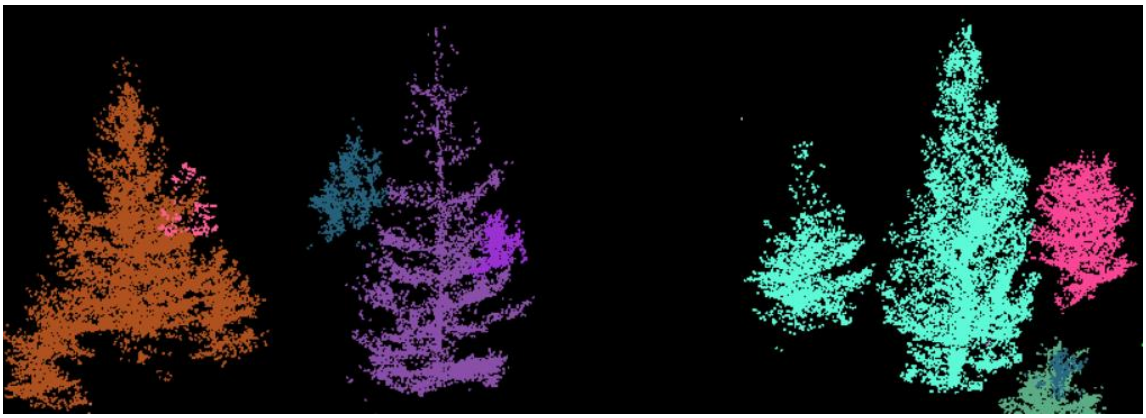

Figure 3-11: Trees segments after connected components and majority filtering

3.3.2. Segment growing

Segment growing uses a set of neighbouring points with similar feature values as seeds (Vosselman, 2013). The seeds are grown by checking if neighbouring points have similar values to the average value of the segment. It makes use of a tolerance which is applied on the average value of the segment to control whether or not a point is added to the segment. Segment growing algorithm is particularly suitable for non-planar segments (Vosselman, 2013). A segment growing algorithm based on roughness was done on the remaining point set. Roughness was used as an attribute for growing because it separates objects with high roughness values from those with low roughness values. Therefore grouping points with this attribute was found to be suitable. The results of the segment growing contained correctly detected points for the ground so this was kept apart. We use the term ground to mean parts of the terrain outside the landslide area. Connected components algorithm is good for points that belong to the same object (Vosselman, 2013). As a result, it was used to group the remaining points on the landslide and low laying vegetation. These were the points with a high roughness value.

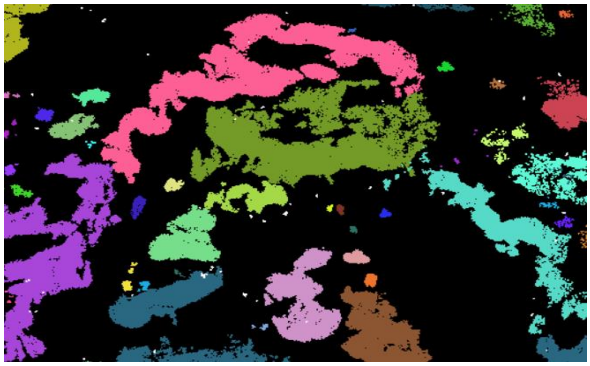

Figure 3-12: Segments on the scarp and landslide boundary with high roughness value.

Majority filtering algorithm is suitable for post processing usually to assign points without segments to nearby segments. These points will typically be assigned to a segment that is most frequent within a defined radius. The output from connected component algorithm and the ground segment were combined and majority filtering applied to assign unsegmented points to a segment. Eventually, the segments of the ground, low laying vegetation, landslide and trees were combined to form final segmentation results. This strategy is shown in Figure 3-13.

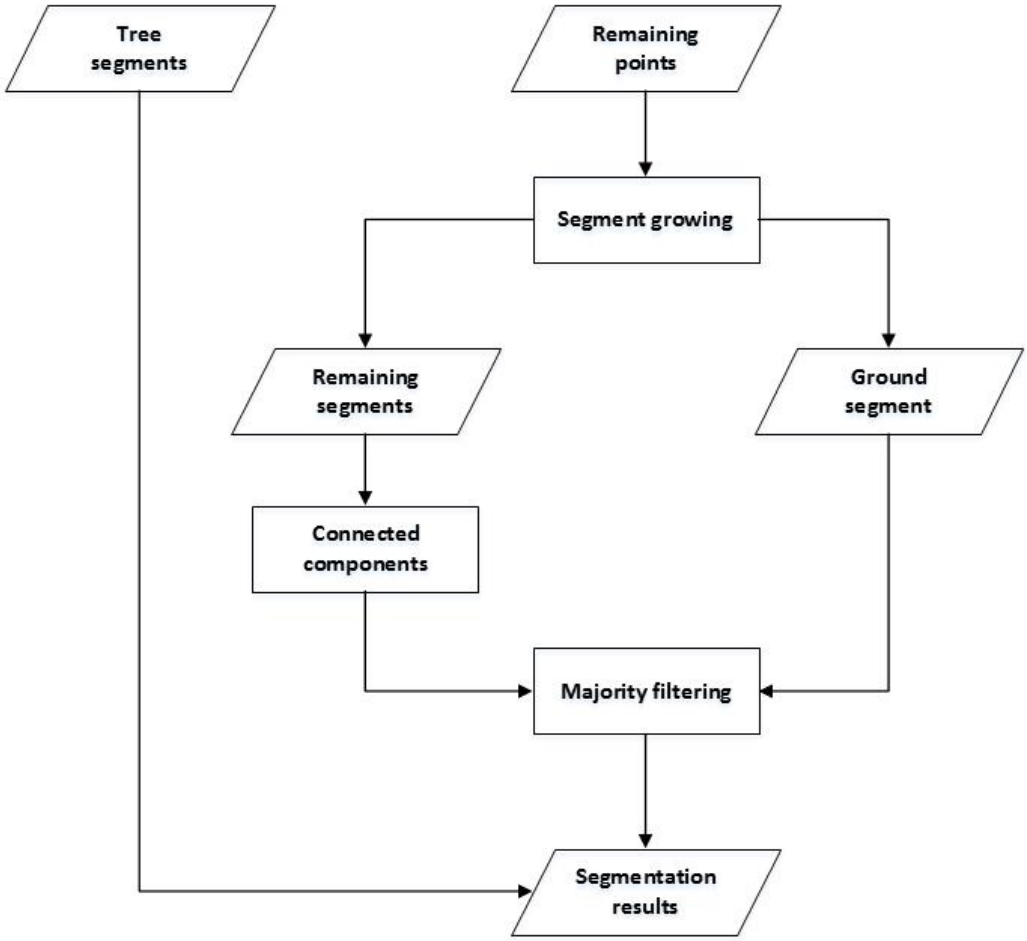

Figure 3-13: Workflow showing the segmentation strategy.

3.4. Object to object matching

Object to object matching provides a platform to compare similar objects in different epochs. Xiao et al. (2012) used the location of trees to match trees in different epochs in order to calculate the change between them. In this study, we used two separate criteria to match similar objects in different epochs i.e. the object properties calculated as point attributes and the minimum distance. The object properties were used as a criterion because we made an assumption that corresponding objects have similar properties. The minimum distance was used because our study area is made of shallow landslides that are characterised by slow movement therefore with this criterion we can expect to obtain corresponding segments. For the matching process, an assumption was made that there is a one to one relation between segments/ objects in one epoch with corresponding ones in the other epoch. Each segment in the first epoch was compared with all segments in the second epoch based on some criteria. The objects we expected for a shallow landslide were the scarp and the main body because the rest of the objects of a landslide were not easily identifiable.

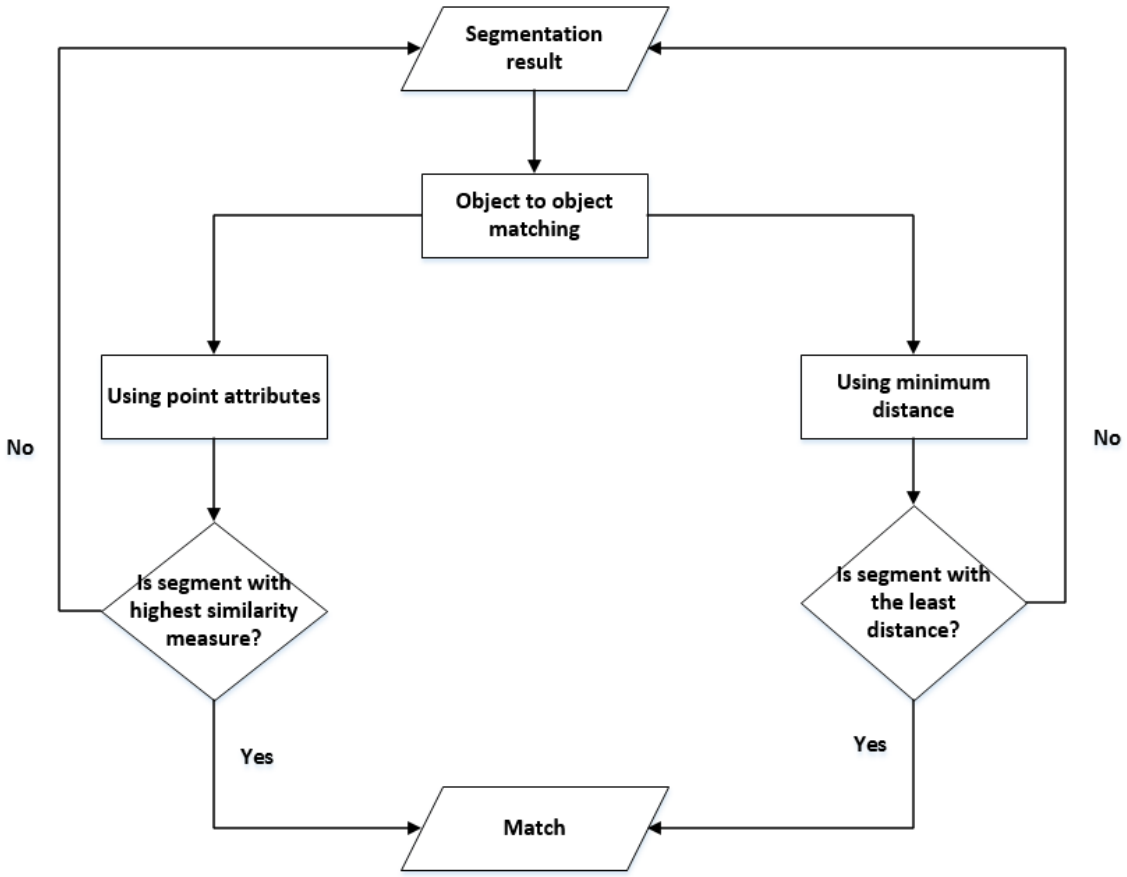

Figure 3-14: Flow of the matching process.

3.4.1. Matching using point attributes

Different point attributes were used independently to see which of them obtained a better match. For each segment, a mean value of the attribute value was computed. A similarity measure was used as criterion for matching. A segment was matched to another in the other epoch if it had the highest similarity measure. The similarity measure was defined as follows:

Similarity measure = 1 - fabs(mean attributevalue1- mean attributevalue2)/(mean attributevalue1+ mean attributevalue2)

Where mean attributevalue1 and mean attributevalue2 correspond to the mean of a given attribute for a segment in epoch 1 and mean of a given attribute for a segment in epoch 2 respectively.

3.4.2. Matching using minimum distance

For each segment in epoch 1, a point to point distance with each segment in epoch 2 was calculated. For each segment in epoch 2, its lowest point to point distance with the segment in epoch 1 was assigned as its lowest distance to the segment in epoch 1. Thereafter all the segments in epoch 2 were assessed to find out which of them had the lowest distance to the segment in epoch 1. Once this was found, it was taken as a match for the segment in epoch 1. This was done iteratively for all segments in epoch 1 in order to find matching segments for them in epoch 2.

3.5. Surface separation distance

Figure 3-15 shows the workflow that was followed when computing the separation distance between two epochs. In this section we describe how the separation distance was computed and how percentages per segment were computed to show parts of the landslide that are dynamic and static.

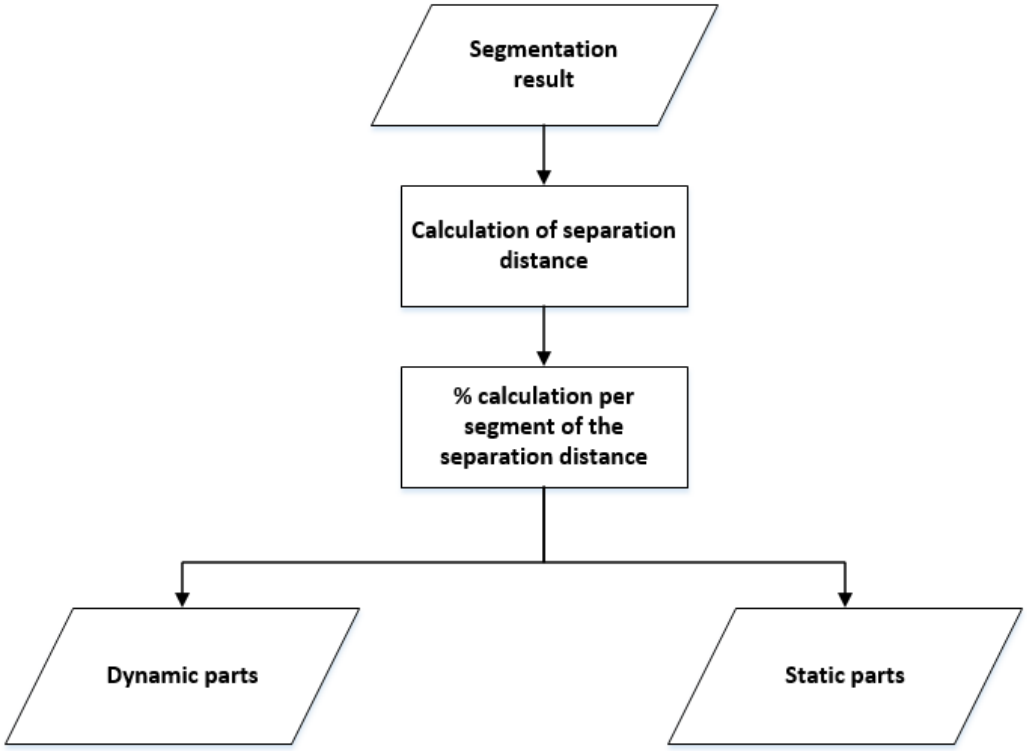

Figure 3-15: Workflow showing how the separation distance is computed and used.

We adopted the workflow shown in Figure 3-15 because when we tested the use of a threshold, the output was a binary map showing values for the surface separation map below and above the threshold. Grouping of points based on similarity of values for the surface separation distance didn't prove as fruitful as well. It was because all the values within in a given tolerance will be group into a segment and yet it's possible that an object could have varying values for the surface separation distance. Consequently, we used the workflow shown in Figure 3-15 that makes use of the segmentation results and thereafter uses the surface separation distance to show how much change was taking placing in each segment.

3.5.1. Calculation of the surface separation distance

The surface separation distance between two epochs was computed as a point attribute. For each point, its neighbours within a given range were defined. The nearest point in the other epoch was then identified. For that point, its nearest neighbours were found and a plane fitted through them. The point to plane distance was then calculated. This was done iteratively for all the points. Thereafter a threshold was defined to show dynamic and static parts of the landslide.

3.5.2. Object based change detection

In order to show whether segments were static or dynamic, the percentage of points whose surface separation distance values were greater than a given threshold was calculated per segment. This percentage was calculated per segment as follows:

Percentage = [(number of points with a surface separation distance greater than a given threshold)/ (total number of points with a surface separation distance)]* 100

3.6. Summary

Our approach starts by identifying what are the properties that describe objects in a landslide. Thereafter, which of these properties can be derived from point clouds? The task was then to decide which of these properties were appropriate for segmentation and at what stage in the segmentation process were they relevant. The matching process was to compare objects in the different epochs. The task was to find appropriate criteria to match these objects. Thereafter, how much change was taking place was investigated. The surface separation distance was also used to show much change was happening in the landslide area.

4. RESULTS AND DISCUSSION

4.1. Introduction

The proposed methodology was tested on three terrestrial laser scanner datasets for two shallow landslides located in Schmirntal, Austria. Section 4.1 describes the datasets and the study area. Section 4.2 shows how the computed point attributes vary across the study area. Section 4.3 shows the results of segmentation and filtering of the data. Section 4.4 describes how segments in two epochs were matched. Section 4.5 describes how the surface separation distance was used to show dynamic and static parts of the landslide.

4.2. Data sets and study area

The data used in this research was for a hill located in the region of Schmirntal in Austria. The data contained two landslides i.e. a large and a small landslide. The datasets were acquired using an Optech ILRIS 3D in October 2011, 2012 and 2013 respectively. Their average point densities are 1770 points/m², 655 points/m² and 664 points/m² respectively.

To make the point processing much faster, the 2011 dataset was thinned by a factor of 2; this means the points were halved. Eventually average point density of approximately 885 points/m² was used. The 2012 and 2013 datasets were not thinned as they were not too large. The data was then cropped into points for the large and small landslides respectively using Cloud Compare software.

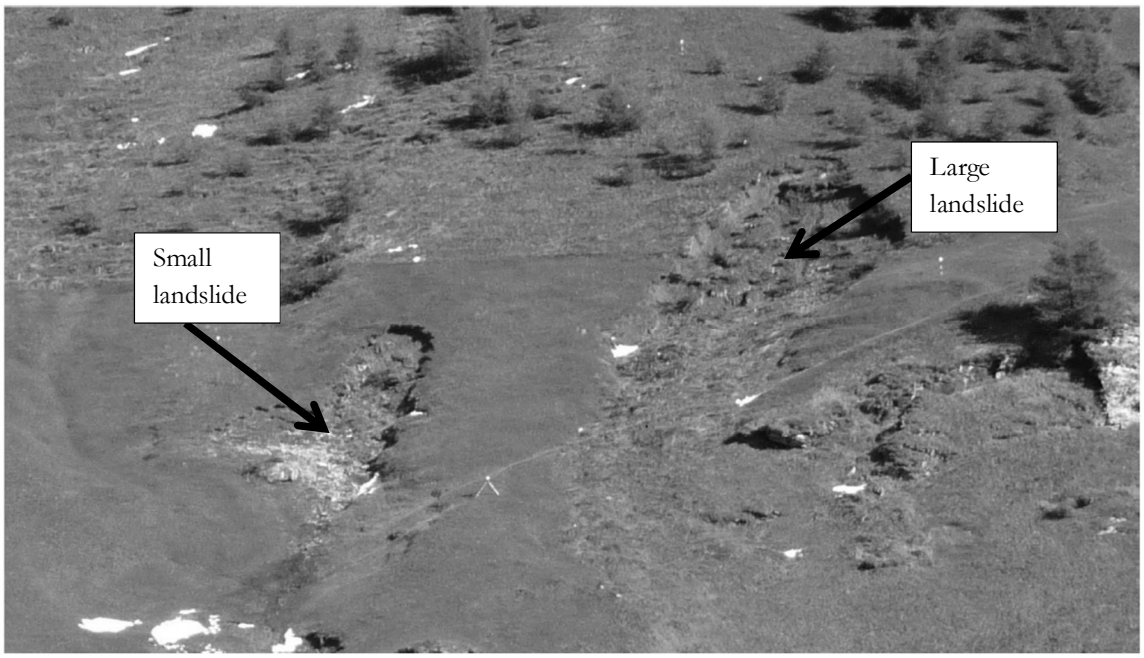

Figure 4-1: Study area in Schmirntal

4.3. Registration

The assumption that point clouds are always correctly registered was not valid for the datasets used in this thesis. Before the methodology was implemented, the tilt observed in the point clouds was eliminated by registration of the different epochs. This was implemented using CloudCompare software. The 2011 point cloud was used as the model to which the 2012 and 2013 point clouds were registered respectively. Figure 4-2 shows the parameters that were used during the registration process.
Different sets of transformation parameters were used to register the 2012 and 2013 point clouds respectively. These parameters are shown in Table 4-1 and Table 4-2.

Table 4-1: Transformation parameters for 2012 point cloud.

1.000	0.003	0.004	0.174
-0.003	1.000	0.007	0.106
-0.004	-0.007	1.000	-0.270
0.000	0.000	0.000	1.000

Table 4-2: Transformation parameters for 2013 point cloud.

1.000	0.001	-0.011	-0.181
-0.001	1.000	0.000	-0.087
0.011	-0.000	1.000	0.450
0.000	0.000	0.000	1.000

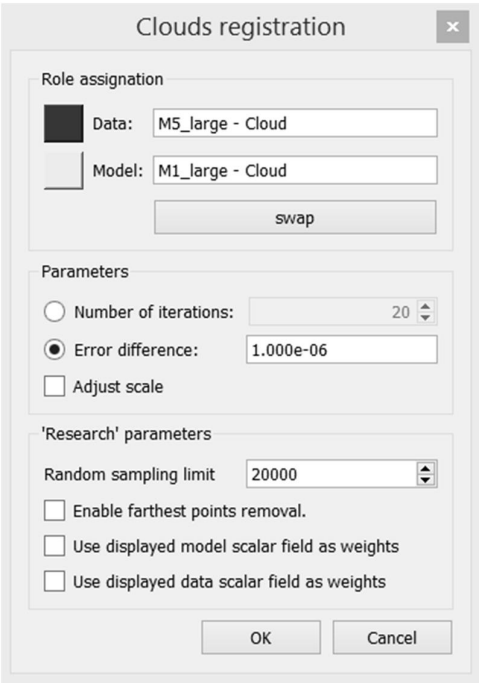

Figure 4-2: Registration parameters.

The distance between point clouds was calculated using CloudCompare before and after the registration to visualise the effects on the tilt and the results are shown in Figure 4-3 and Figure 4-4.

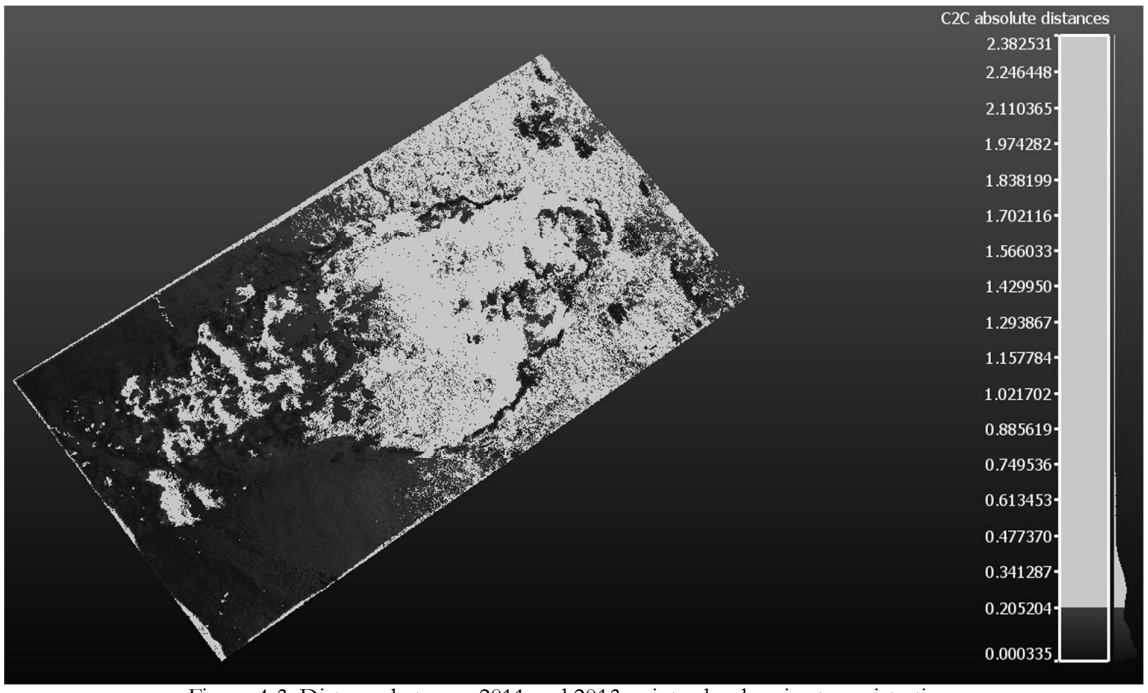

Figure 4-3: Distance between 2011 and 2013 points clouds prior to registration.

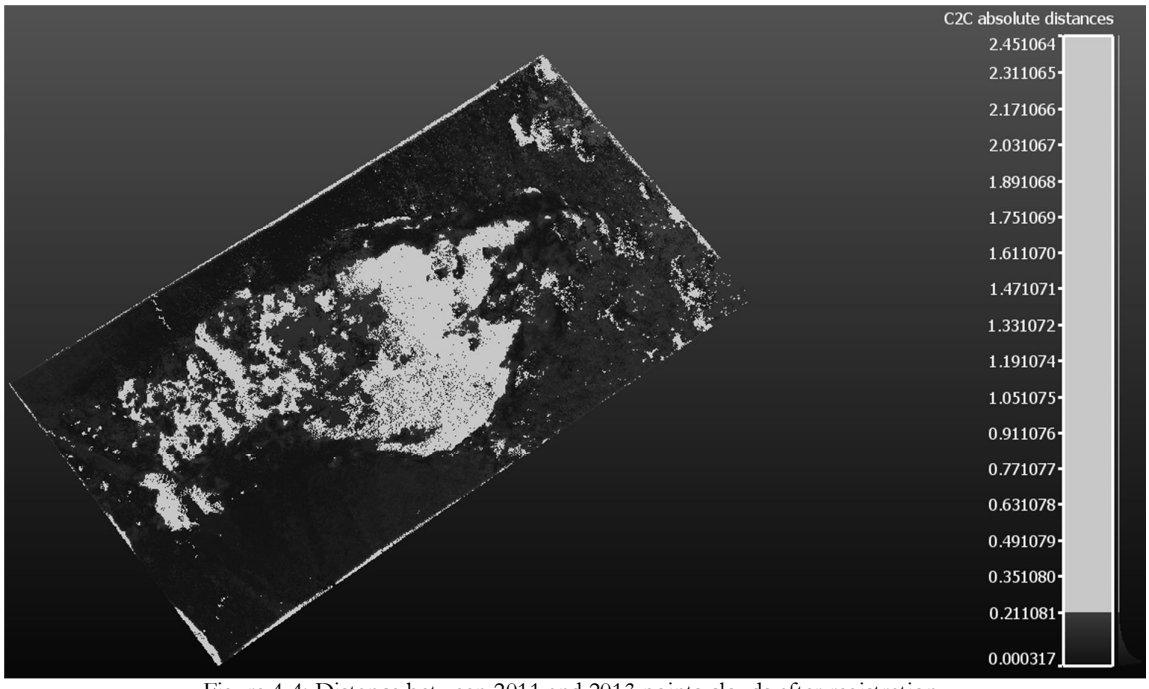

Figure 4-4: Distance between 2011 and 2013 points clouds after registration.

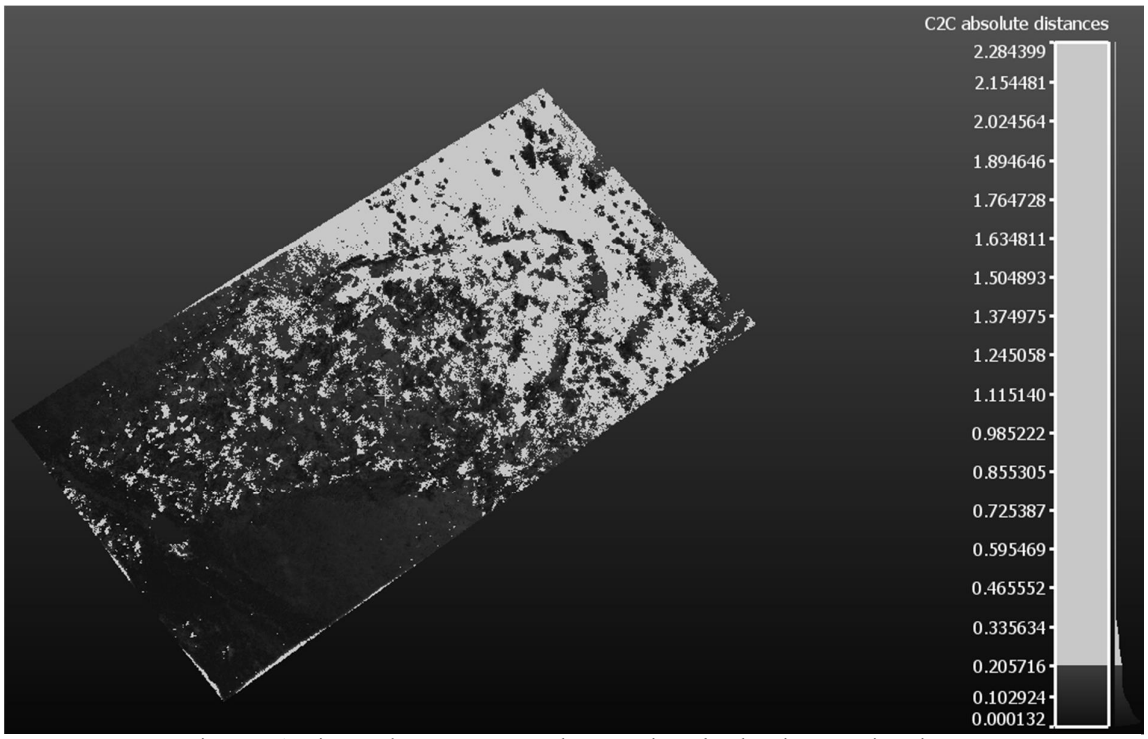

Figure 4-5: Distance between 2011 and 2012 points clouds prior to registration.

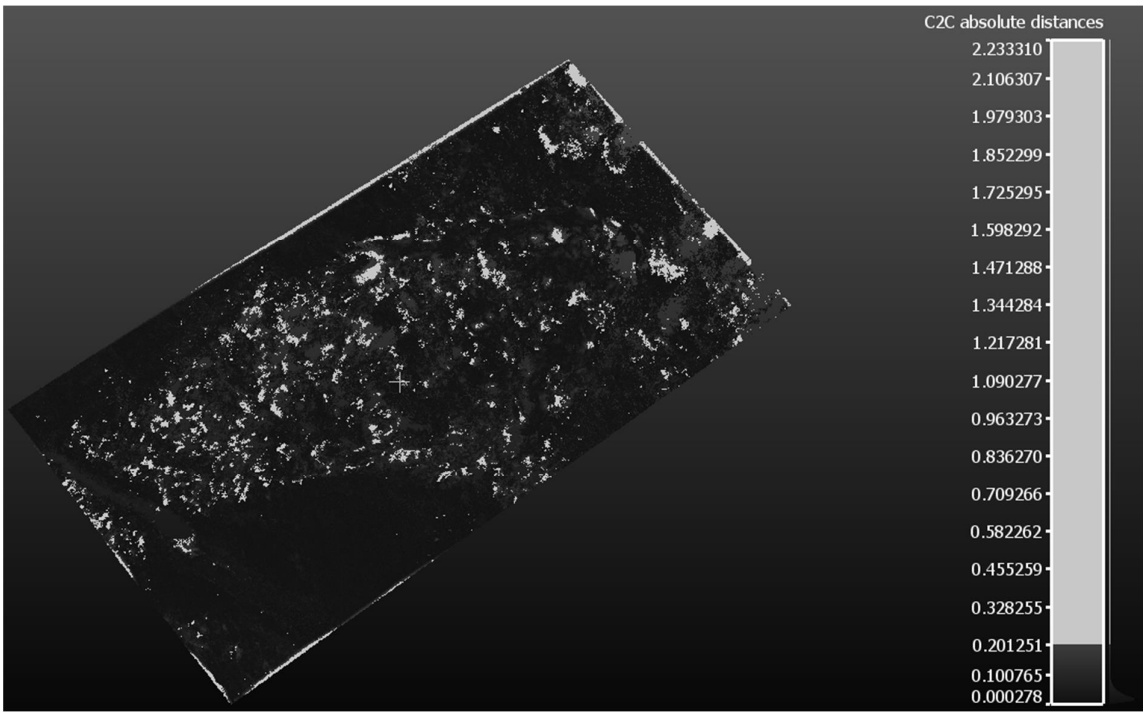

Figure 4-6: Distance between 2011 and 2012 points clouds after registration.

In Figures 4-3 and 4-5 systematic effects of the tilt were observed in the upper parts of the point clouds. Points on the terrain were seen to have high values like points on the trees which is not the case in reality but the effects of the tilt. With the tilt removed after registration as shown in Figures 4-4 and 4-6, these systematic effects were eliminated. It was observed that points on the terrain had approximately even values through the point cloud with trees and parts that are changing having high values. The systematic effects of the tilt observed in Figures 4-3 and 4-5 were due to a poor distribution of the targets that were used to register the data initially. The results shown in Figures 4-4 and 4-6 showed that our approach was an improvement to the approach that was used earlier when the data was collected. The systematic effects due to tilt were significantly reduced which gave more confidence to computation calculated on these points thereafter.

4.4. Segmentation

4.4.1. Separation of points on trees and low laying vegetation

Before a connected components analysis was done, the points on the trees were separated from the rest of the points. The point attributes of height above lowest local point and height difference were observed to have high values on trees and low laying vegetation as shown in Figure 3-3 and 3-4 respectively. Therefore they were used to separate the points on trees and low laying vegetation from the rest of the points.
A selection was made on points with height above local point values greater than or equal to 0.5m. This value was reached at through several trials. Figure 4-7 shows the result of this selection. Points with values for the height above lowest local point less than 0.5m are shown in Figure 4-7(a) while those greater than or equal to 0.5m are shown in Figure 4-7(b). Most of the points belonging to the terrain are retained as shown in Figure 4-7(a) and likewise all points on trees and low laying vegetation are also captured as shown in Figure 4-7(b). However some points on the terrain were found to have values greater than or equal to 0.5m. Some of these points are shown using the red circles in Figure 4-7(b). These points are likely due to the low value of the threshold chosen to accommodate all points on the tree.

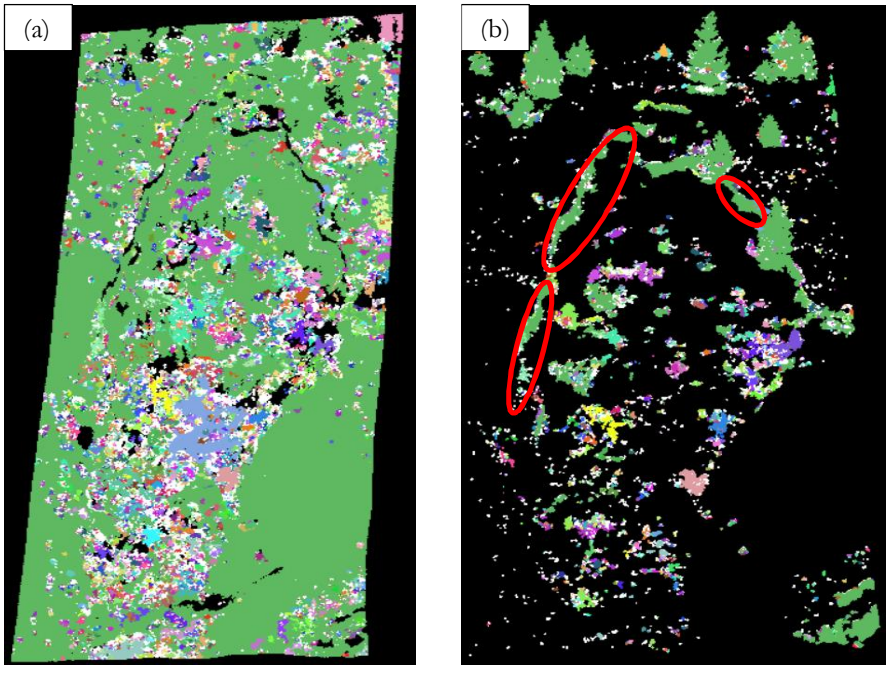

Figure 4-7: Points with values less than 0.5m for the height above lowest local point (a) and (b) are points with values greater than or equal to 0.5m

In order to separate these remaining terrain points from points on trees and low laying vegetation, the point attribute of height difference was used. The reasoning behind the use of this attribute at this stage was that points on terrain will have smaller values as compared to points on trees and low laying vegetation. A value of 1.3m was found to be an optimal value for this attribute to use to distinguish between the points on the terrain and the points on trees and low laying vegetation. This value was reached at through several trials. A selection was made on points with values for the height difference greater than 1.3m. This captured the points on trees and low laying vegetation as shown in Figure 4-9. The rest of the points with values less than or equal to 1.3m as shown in Figure 4-8 were combined with the result in Figure 4-7(a) to eventually have points on the terrain. This result was kept and later used in the segment growing stage

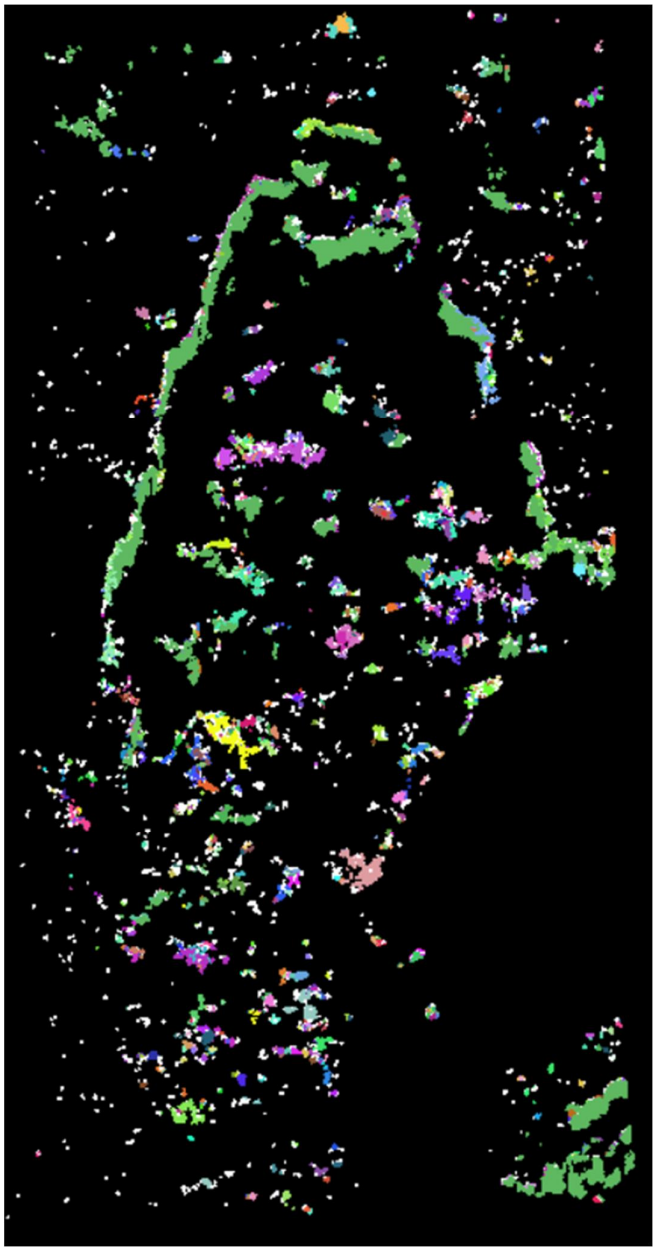

Figure 4-8: points with values for the height difference less than or equal to 1.3m

Generally all points on trees and low laying vegetation were captured. However, there were still a few points that belonged to the terrain that were not removed by the previous selection on points using the height above lowest local point and height difference point attributes. These points are shown by the grey circles in Figure 4-9. Their presence can be explained by the fact that using a threshold is not always precise. These points were grouped into objects and the results are shown in Appendix 1.

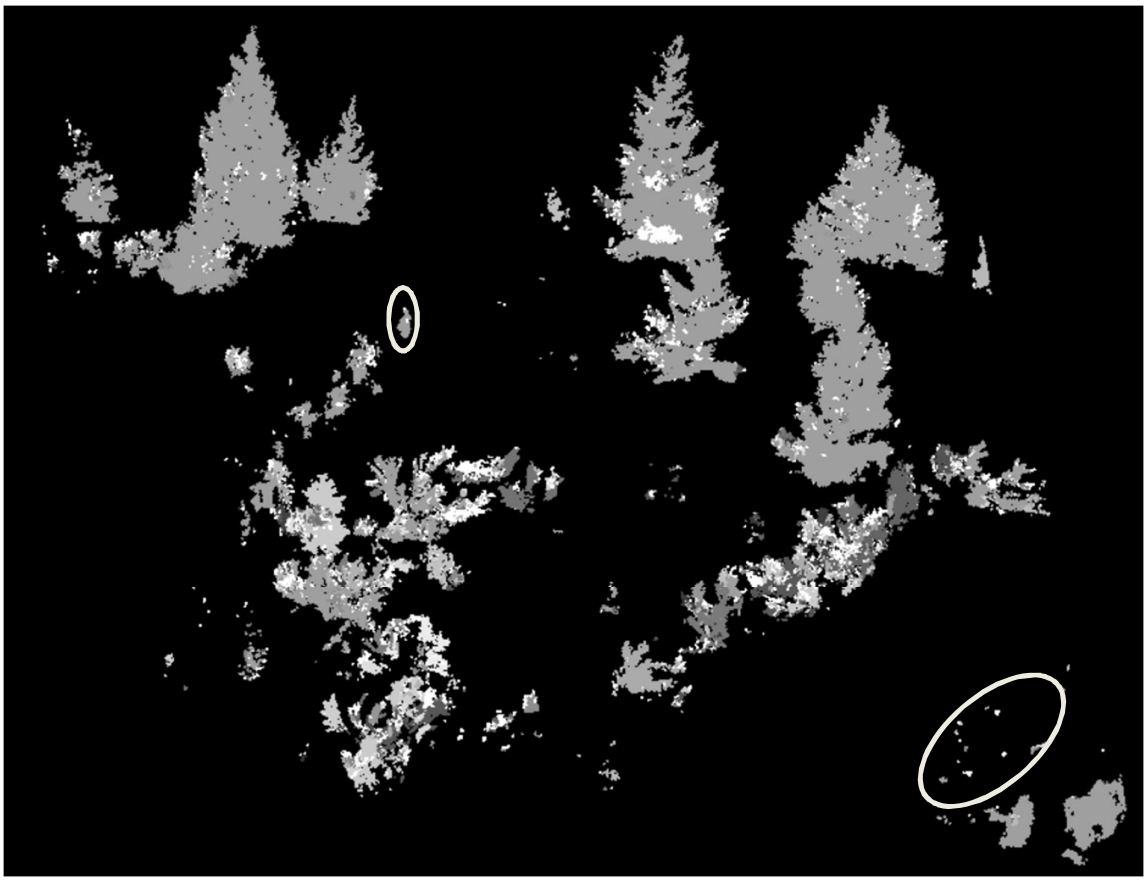

Figure 4-9: Points with height difference values great than 1.3m and height above lowest local point values greater than or equal to 0.5m.

4.4.2. Segment growing

A segment growing based on roughness at a tolerance of 0.05m was done to distinguish between the low laying vegetation, ground and sub-objects of the landslide. The results of this segmentation are shown in Figure 4-10.

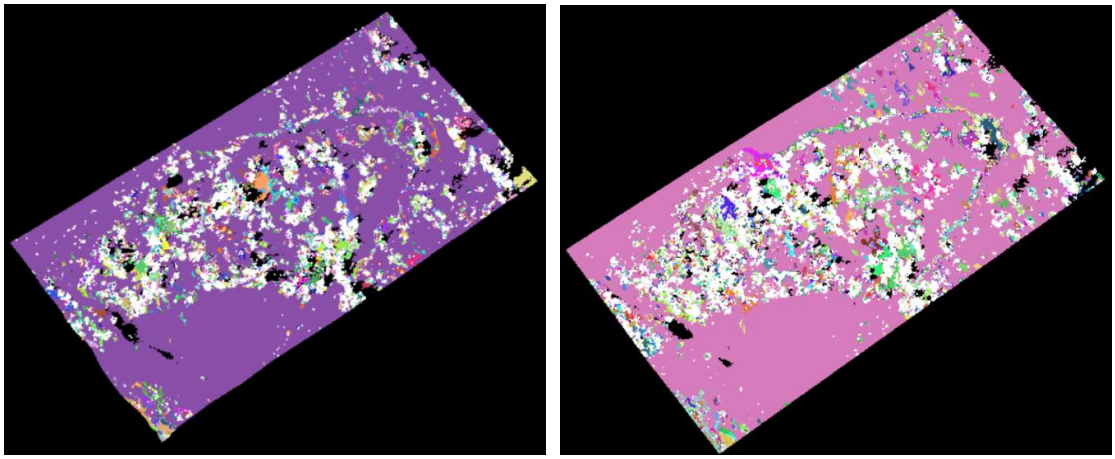

(a) (b)

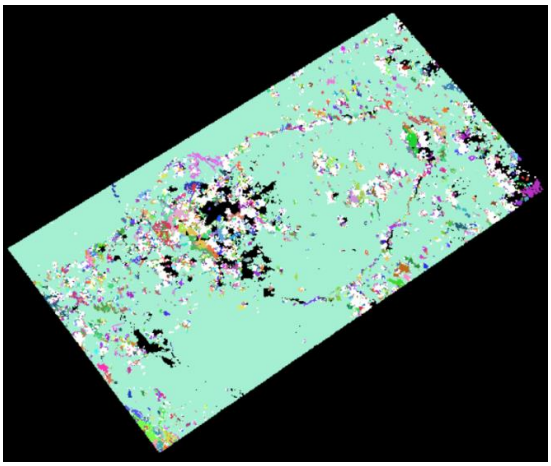

(c)

Figure 4-10: Segment growing results (a) 2011, (b) 2012 and (c) 2013.

Generally, most points on the ground were grouped together as a large segment. Non-segmented points were observed on the boundary of the landslide and some low laying vegetation. These were points which didn't have neighbouring points with similar feature values to start a new seed. The large segment was kept away and connected components analysis was done on the remaining points as shown in Figure 4-11. As a result, the small segments previously seen in Figure 4-10 were grouped into larger segments. Points on the boundary of the landslide were grouped into clear segments. However, some unsegmented points (white points) were still observed as seen in Figure 4-11. These were points which didn't meet the maximum distance criterion used during connected components analysis. This criterion was 1m. This output was combined with the previously kept large segment and a majority filter was used to assign these points to a segment. Points were assigned to a segment if it was the most frequent in a neighbourhood radius of 1m. The output was final segmentation results shown in Figure 4-12. This entire procedure was repeated for all the datasets i.e. 2011, 2012 and 2013.

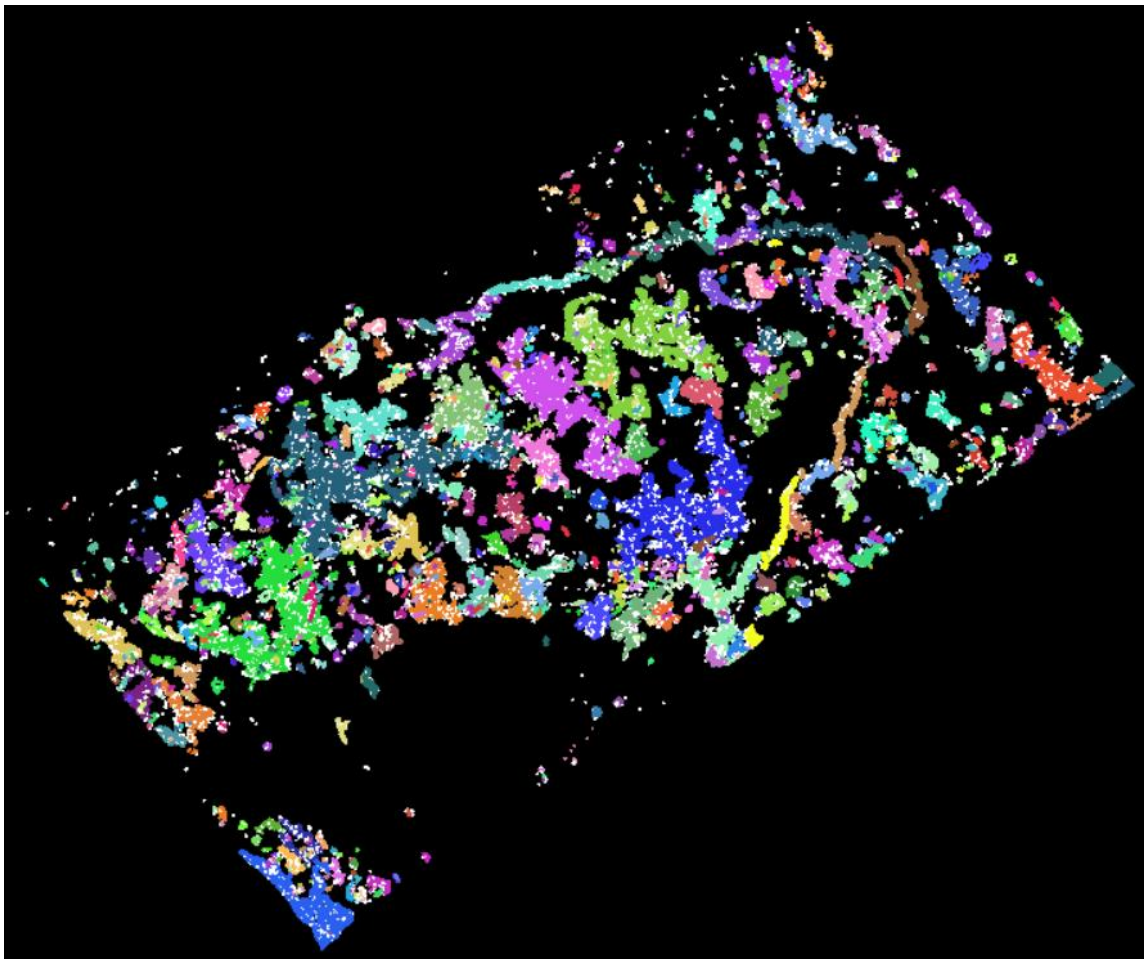

Figure 4-11: Connected components on points of 2011 large landslide.

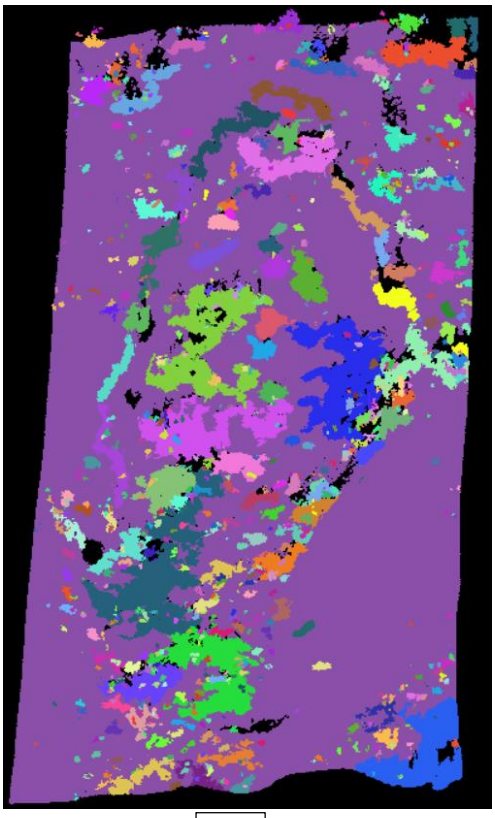

(a)

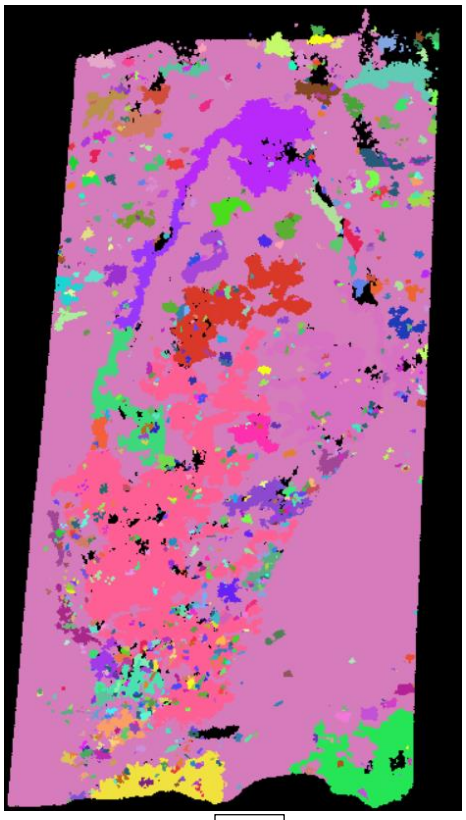

(b)

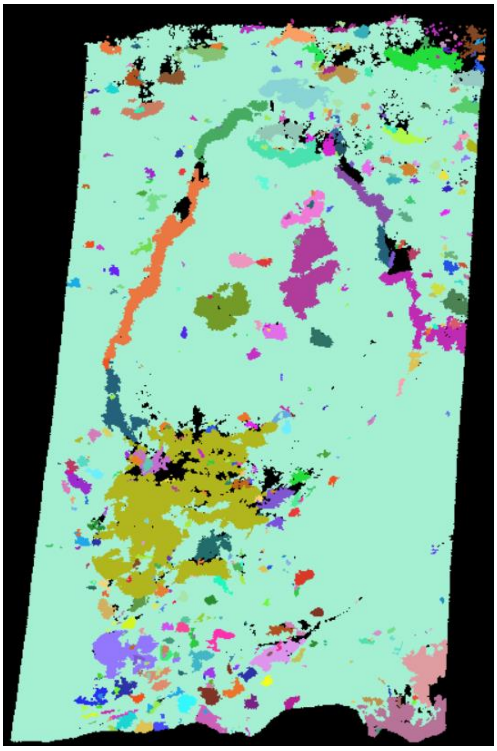

(c)

Figure 4-12: Final segmentation results (a) 2011, (b) 2012 and (C) 2013.

The final segmentation results were obtained for the three epochs used in this study i.e. 2011, 2012 and 2013 as shown in Figure 4-12. The segmentation results in Figure 4-12 showed that the large ground segment correctly contained only points on the ground. The boundary of the landslide was segmented into many parts. This is likely due to those segments having different feature values than for neighbouring segments. Some patches of low laying vegetation were correctly detected. Over segmentation around the scarp area was observed at the scarp area for the 2011 and 2013 epochs as shown in Figure 4-13. The 2011 data however shows a better segmentation result for the scarp although it also appears to be under segmented. This irregular pattern could be linked to the difference in feature values around the scarp for the different epochs.

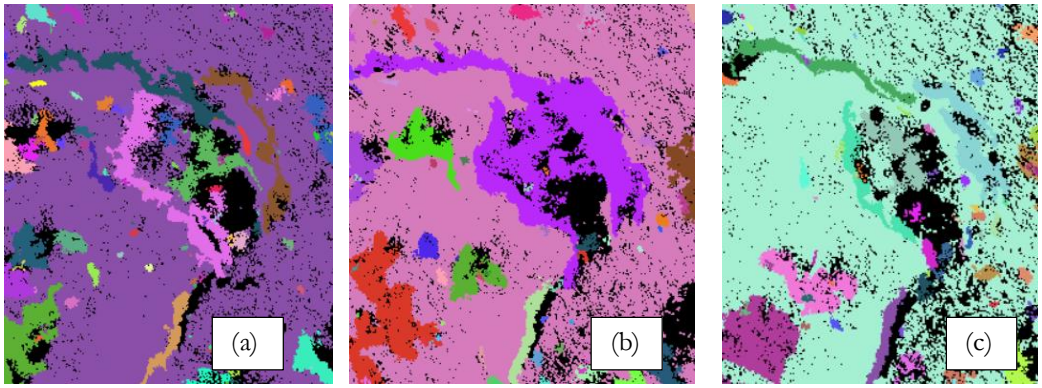

Figure 4-13: Scarp area for 2011 (a), 2012 (b) and 2013 (c) data.

In the segmentation results for the 2011 epoch, over segmentation was observed along the boundaries of the landslide especially on the upper part of the landslide. At the bottom, the boundary was merged with the large ground segment. This was probably because of the similarity of feature values along that part. Within the landslide area, very many small segments were seen especially at the bottom. This was probably because in the initial segment growing phase points in these segments had distinct feature values as compared to those of neighbouring points. Even after applying the connected components they were not merged into larger segments because they didn't meet the distance threshold of 1m used in the connected components segmentation. Similarly, the segmentation results of the 2013 epoch showed over segmentation along the boundaries of the landslide. Small segments were also observed on the ground. This was because these points had feature values that were different from those of neighbouring points therefore they were group into separate segments. In contrast, the segmentation results for the 2012 epoch showed the scarp and part of the landslide boundary merged into a single segment. This was because in the initial segment growing segmentation, these points had distinct feature values so they formed small segments. However, when connected components was applied, they were all grouped into a large segment since these segments were close by and the criterion for grouping into a segment was based on a distance threshold. In comparison with the 2011 and 2013 segmentation results, the 2012 results were poor.

4.4.2.1. Influence of segmentation parameters

The segmentation parameters i.e. neighbourhood, radius and tolerance were varied to see their influence on the segmentation results. The size of the neighbourhood i.e. number of points in a neighbourhood used to calculate the point attributes was varied for 200, 120 and 100 points. It was observed that the increase in the size of the neighbourhood had no effect on point attribute calculation. This is because the point density of the data is very high such that even if the number of neighbours around a point were increased, they would still be close to the point and would not greatly affect the feature value calculated. However, it was noted that increasing the size of the neighbourhood slows the processing speed. In that case it's good to use a considerable number of points for fast processing. The radius used during point attribute calculation was also varied for 0.3m, 0.5m and 1m. No noticeable difference in the feature values calculated was observed. With increase in the radius, we could still find the number of points for feature value computation within a small radius for the point in question. This is likely due to the high point density of the data. When the tolerance for the attribute used for segment growing was altered, it was observed that for a large tolerance, most of the points were merged into large segments. This was because the feature values between most of the neighbouring points were not too distinct. However, a very low value could also lead to over segmentation. Therefore, in order to obtain optimal segmentation results, a lower optimal value for the tolerance is suitable although this will also depend on the type of object expected to be extracted.

4.4.3. Discussion

By making use of different segmentation and post processing steps, final segmentation results that group points on the ground, trees, scarp, landslide boundary and low laying vegetation can be obtained. Most trees were grouped into single segments with a few exceptions having two or more segments. Over segmentation on the boundary of the landslide and scarp area is due to some points having very different feature values than those of surrounding points. The point attribute used can either be derived in a single or multiple epochs depending on what object or characteristic of an object is of interest. The shape of the neighbourhood used in calculating point attributes for the segmentation process should be varied depending on the characteristic/ property of the object of interest. Some object properties like slope and surface separation distance are more suitable to be used for thresholding than as an attribute for segmentation. The segmentation results have to be combined with knowledge of the area or an image of the area in order to obtain full value from them. This is because of the difficulty in interpreting the data on its own. In the absence of reference data, we used a manual interpretation using the knowledge of the data and image of the area to assess the quality of the segmentation. This was done using visual inspection. In such a case ascertaining the quality of the segmentation becomes rather subjective.

4.5. Object to object matching

After the segmentation process, the segments in one epoch were matched to corresponding segments in another epoch. The criteria used for matching was the minimum distance and the highest similarity measure.

4.5.1. Matching using point attributes

With this approach, the criterion used for matching was the similarity measure. This similarity measure was described in section 3.4.1. Segments were matched to each other if they had the highest similarity measure based on a given point attribute. The similarity measure was tested using point attributes of slope and roughness. These attributes were selected because they characterise the objects that were expected to be matched. The results for matching using this criterion were not good. Almost all matches were incorrect. This was probably due to values used in calculating the correlation. These values were calculated

as averages of a particular point attribute per segment. The dynamic nature of the data also made it difficult for the same segment in the different epochs to have similar values.

4.5.2. Matching using minimum distance

Matching based on minimum distance yielded mixed results. Some segments were correctly matched while others were incorrectly matched as shown in Figure 4-14. The green arrows represent correctly matched segments while the red ones represent incorrectly matched segments. The majority of the correct matches were obtained on the small segments. However, with the large segments, incorrect matches were obtained. This inconsistency in matching could be linked to the dynamic nature of the data.

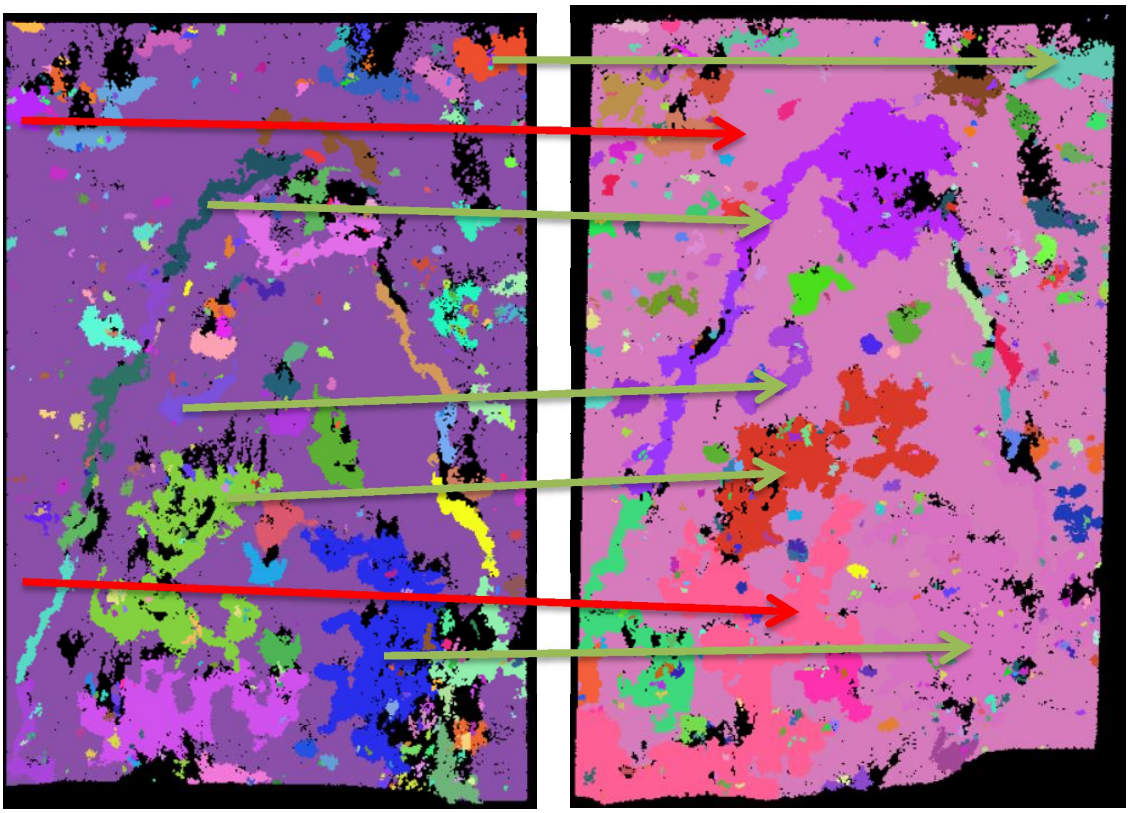

Figure 4-14: Matching results using minimum distance between 2011 and 2012 epochs.

4.5.3. Discussion on matching process

The matching between segments in different epochs could not be correctly implemented with the criteria used. Having said that, relatively some success was obtained with the minimum distance as a criterion for matching. In contrast, the use of point attributes yielded poor results. We also explored the idea of matching using all point attributes per segment but it turned out to be cumbersome and difficult to implement.

The quality of the matching was tested by manually checking for segments that matched. With the criterion of using the similarity measure of point attributes, the quality was poor. On the other hand, using minimum distance showed some good instances of matches between segments although still wrong matches were registered. It must be said that the quality of the segmentation has a bearing on the quality of the matching. With a good segmentation result, the expectation for good matching results is

significantly enhanced. In a scenario where a particular segment/ object in one epoch is either over/ under segmented and a similar one in the other is correctly segmented as shown in Figure 4-15, quantifying change becomes difficult. This is because the correctly segmented object will be matched with all similar over segmented segments in the other epoch.

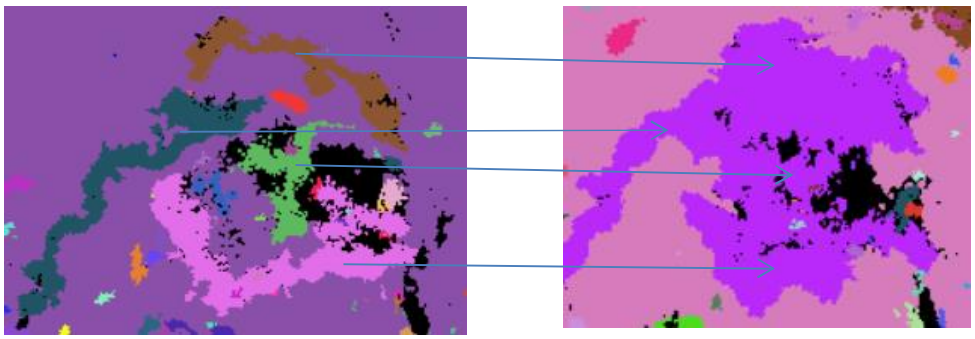

Figure 4-15: Matching result showing several segments matched to one segments.

The knowledge on how the objects move could also be implemented to improve on the matching process. More properties of the objects can be added to the data and used as a matching criterion. This will likely increase the possibility of getting correct matches. The volume of the objects can be used as a measure of change by comparing the volumes of the object in one epoch with another similar one in the other epoch. However, the use of size as a measure of change is likely to yield results that don't make a lot of sense. This is because the size is determined by the segmentation result than by the object itself.

4.6. Surface separation distance

4.6.1. Calculation of surface separation distance

This point attribute was calculated between the 2011 and 2012, 2012 and 2013 and then finally for 2011 and 2013 datasets. First, the 50 neighbours within a range of 3m were found. The nearest point in the other epoch was then identified. For that point, its nearest 20 neighbours were found and a plane fitted through them. The point to plane distance was then calculated. This was done iteratively for all the points. A threshold of 0.3m was used to distinguish between dynamic and static parts of the landslide. This threshold value was used so that the separation distance wouldn't be confused with the registration error. The registration error for the datasets was approximated to be less than 0.2m. Points with values higher than the set threshold were taken as dynamic while those lower than the threshold were taken as static. Dynamic in this case means parts more affected by the landslide while static are parts less affected by the landslide.

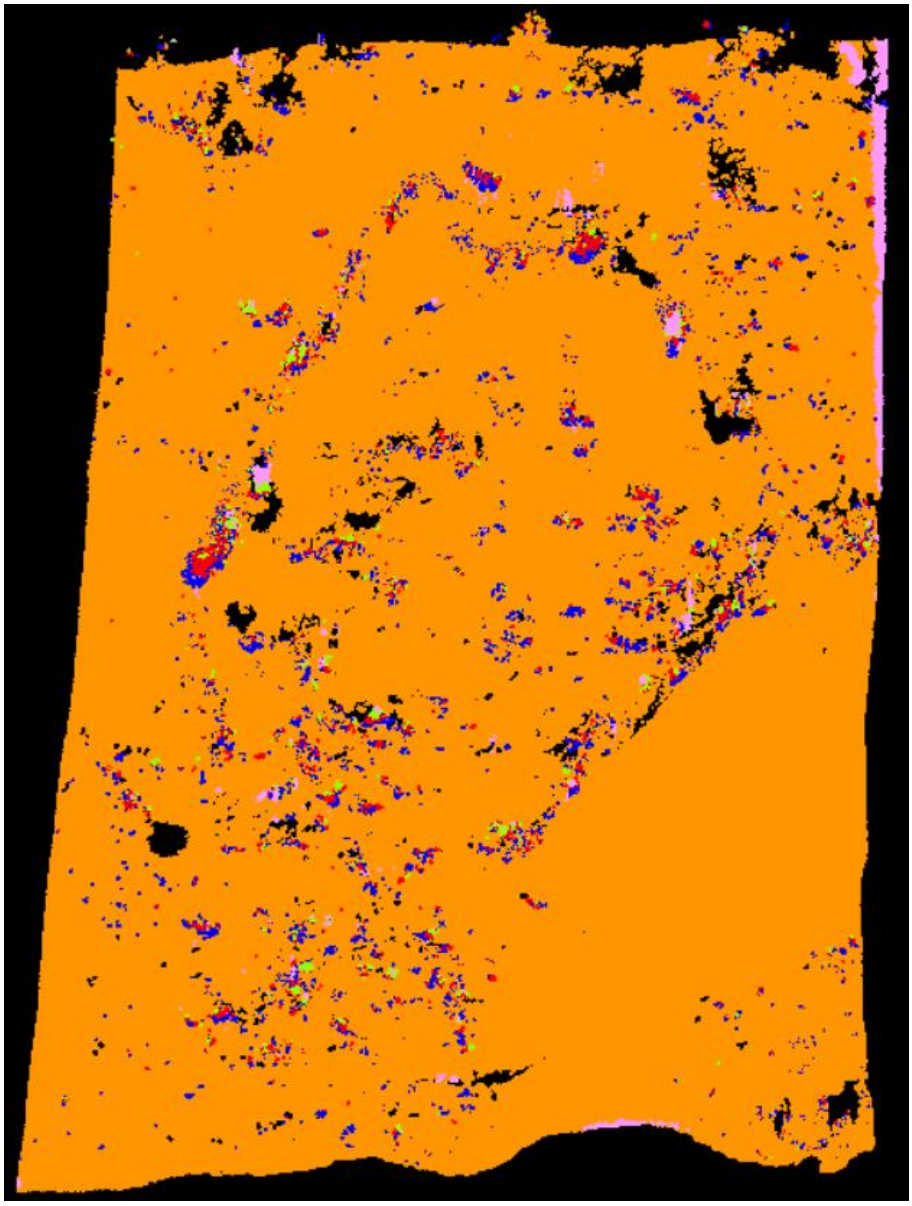

Figure 4-16: Surface separation distance between 2011 and 2012 epochs.

Table 4-3: Colour legend showing colours corresponding to value per point.

Surface separation distance	<0.3m	>0.3≤0.5m	>0.5≤0.7m	>0.7≤0.9m	>0.9m
Colour					
RGB	255 150 0	0 0 255	255 0 0	150 255 0	255 153 255

In Figure 4-16, the values of the surface separation distance for points is shown. Generally most points on the large landslide have values less than 0.3m. This implies that nothing much changed between 2011 and 2012. A few points changed or moved and these are coloured blue, red, green or pink. The few points with large differences (coloured pink) on the top right hand corner are not because of any change but because of the two epochs not overlapping precisely at that point.

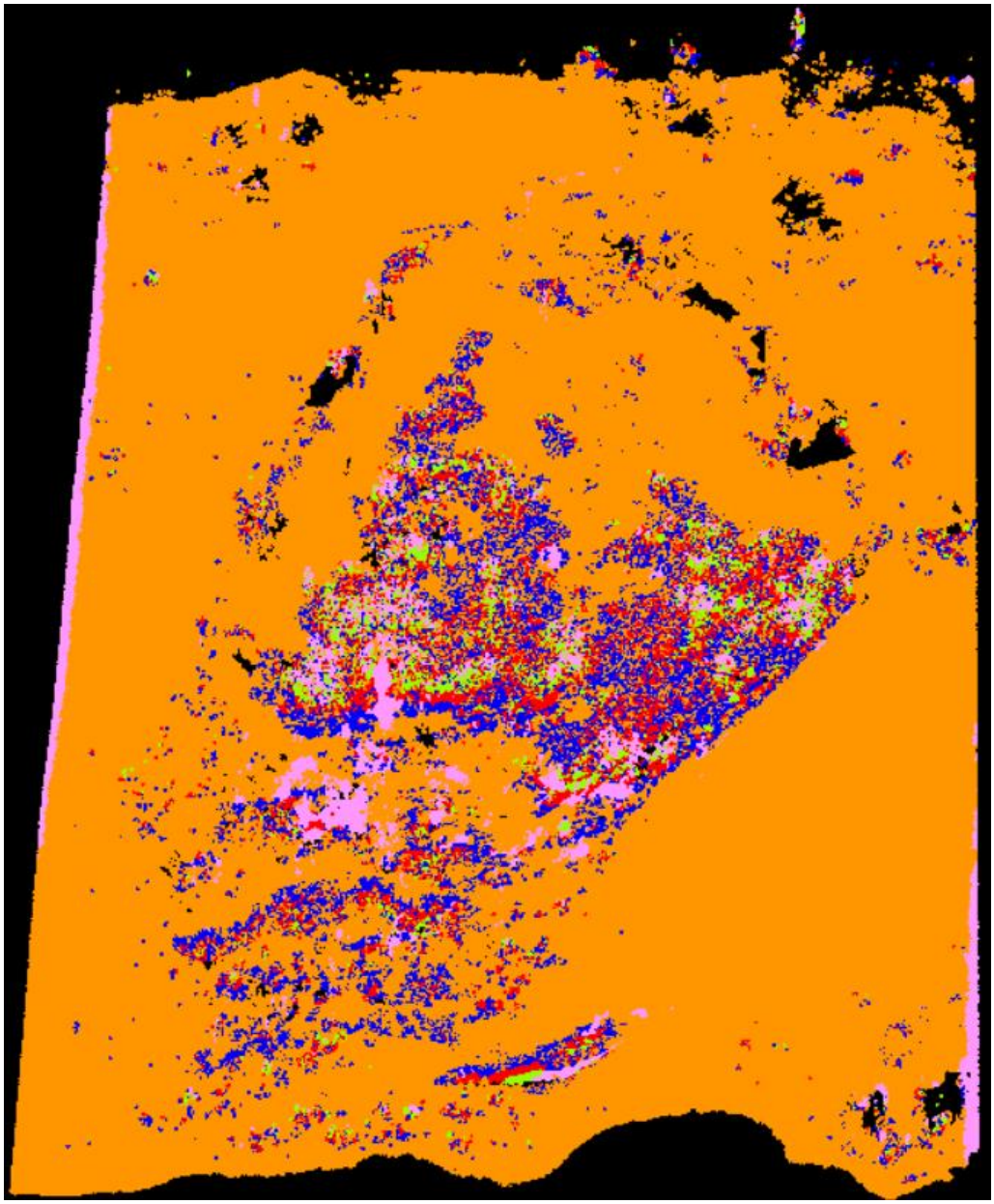

Figure 4-17: Surface separation distance between 2012 and 2013 epochs.

Figure 4-17 shows results for the surface separation distance computed between the 2012 and 2013 epochs. Generally most points of the large landslide had small differences. Large differences were observed within the body of the landslide. This was probably due to something moving or changing within the body of the landslide. A few points at the edges of the epochs were observed to have large differences as well. This was because at those points the epochs didn't precisely overlap. As a result, these points were assigned a value of 3m because no points were found within a range of 3m in the other epoch. The dynamic parts within the landslide were observed to increase as compared to the results in Figure 4-16.

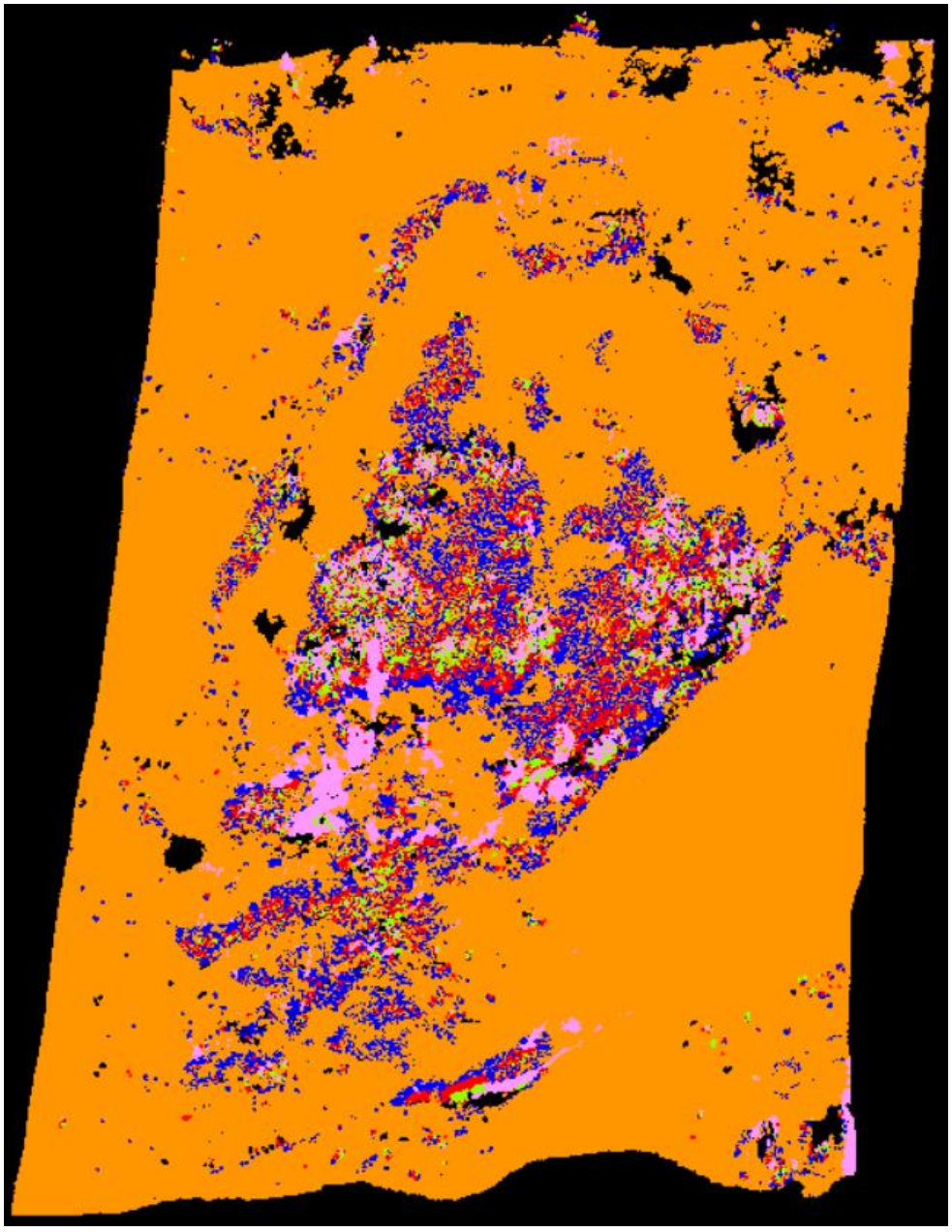

Figure 4-18: Surface separation distance between 2011 and 2013 epochs.

Figure 4-18 shows most of the points with large differences are located within the body of the landslides. A few points were also observed on the boundaries. Most of the points for the surface separation distance calculated between 2011 and 2013 were observed to have small differences. From the results in Figure 4-16, 4-17 and 4-18, it was observed that the points with large differences increased from 2011 to 2013.

4.6.2. Object based change detection

In order to show how much change was taking place per segment, the percentage of points that were dynamic was calculated. Points in each segment that had a surface separation distance greater than 0.3m were defined as dynamic. This was done for all the segments in each epoch.

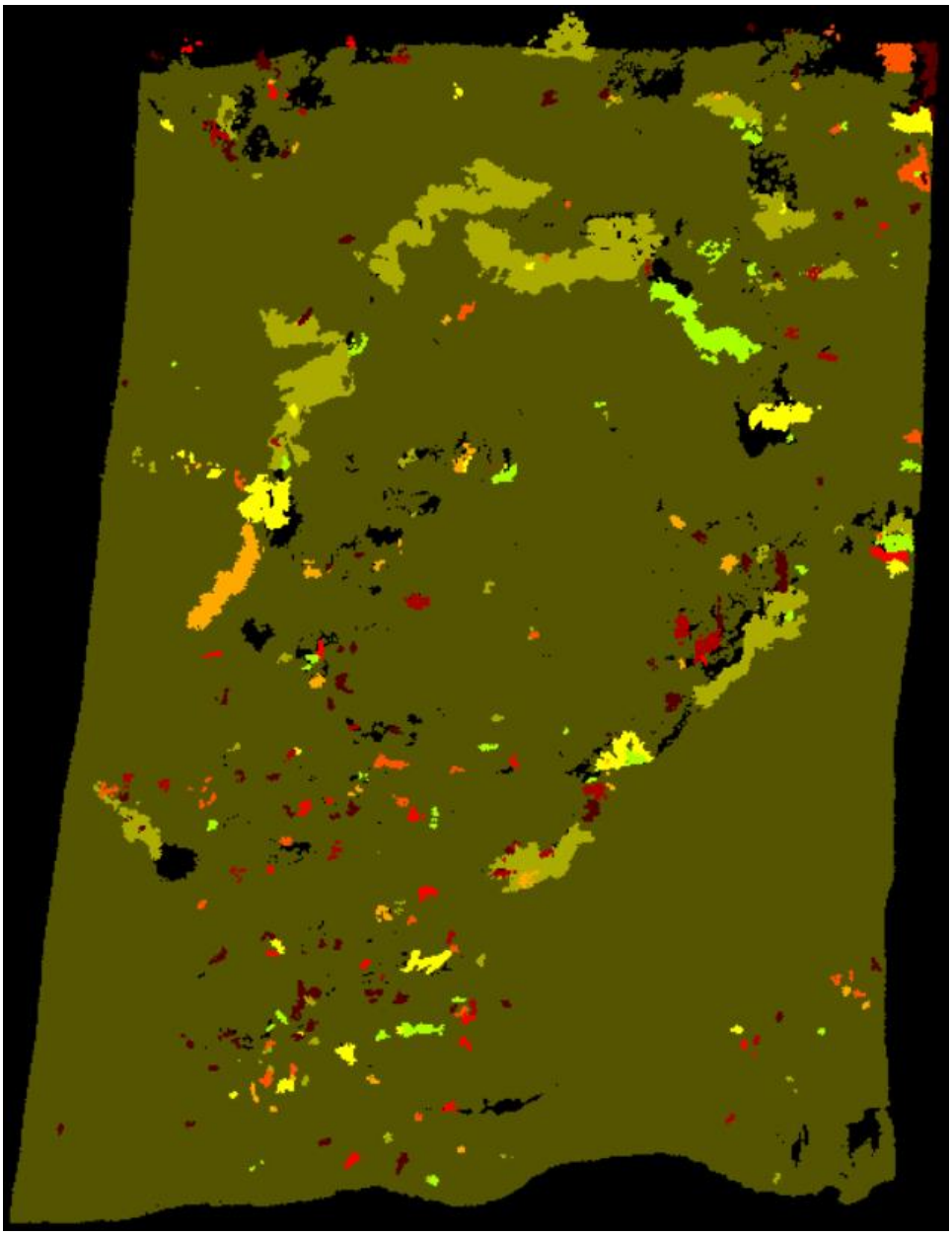

Figure 4-19: Segments coloured according to percentage of points that are dynamic between 2011 and 2012 epochs.

Table 4-4: Colour legend showing colours corresponding to percentages

Percentage	<10	≥10<20	≥20<30	≥30<40	≥40<50	≥50<60	≥60<70	≥70<80	≥80
Colour									

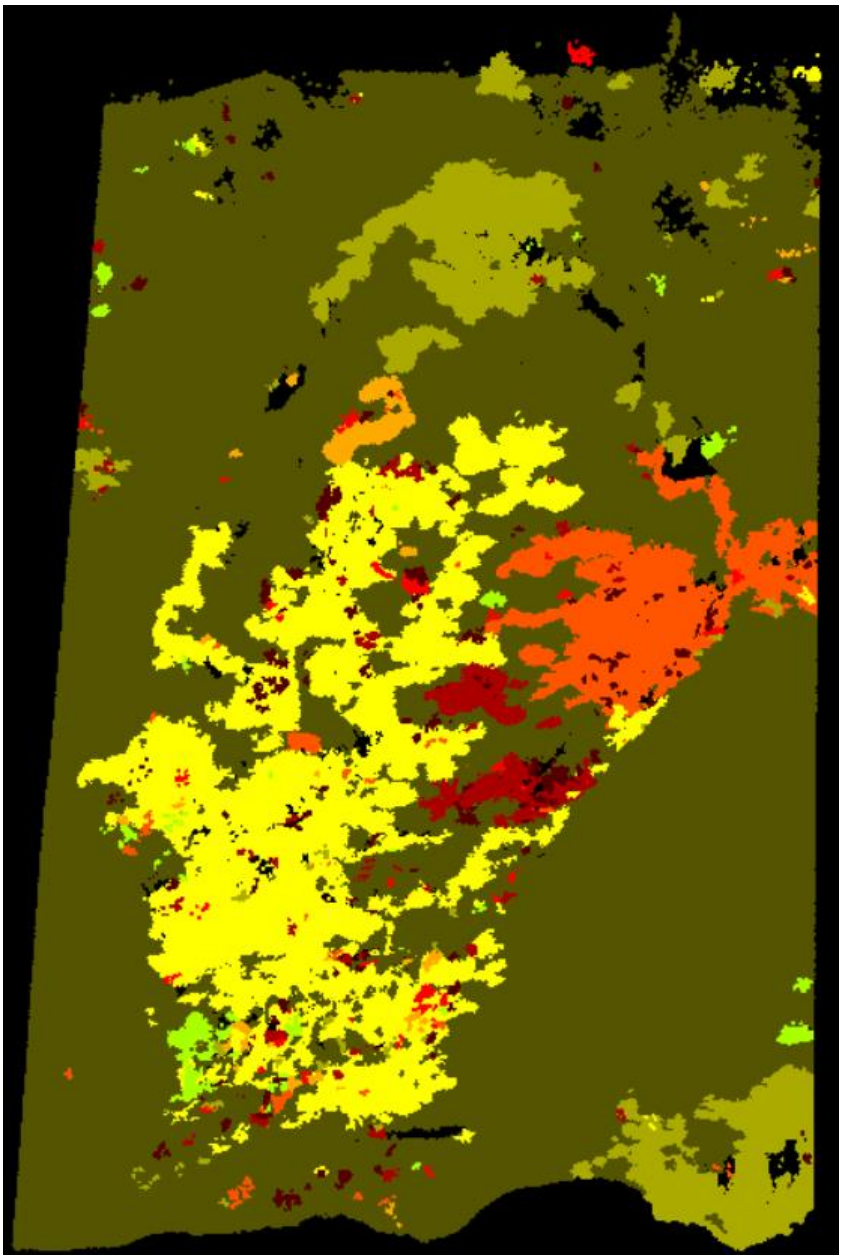

Figure 4-20: Segments coloured according to percentage of points that are dynamic between 2012 and 2013 epochs.

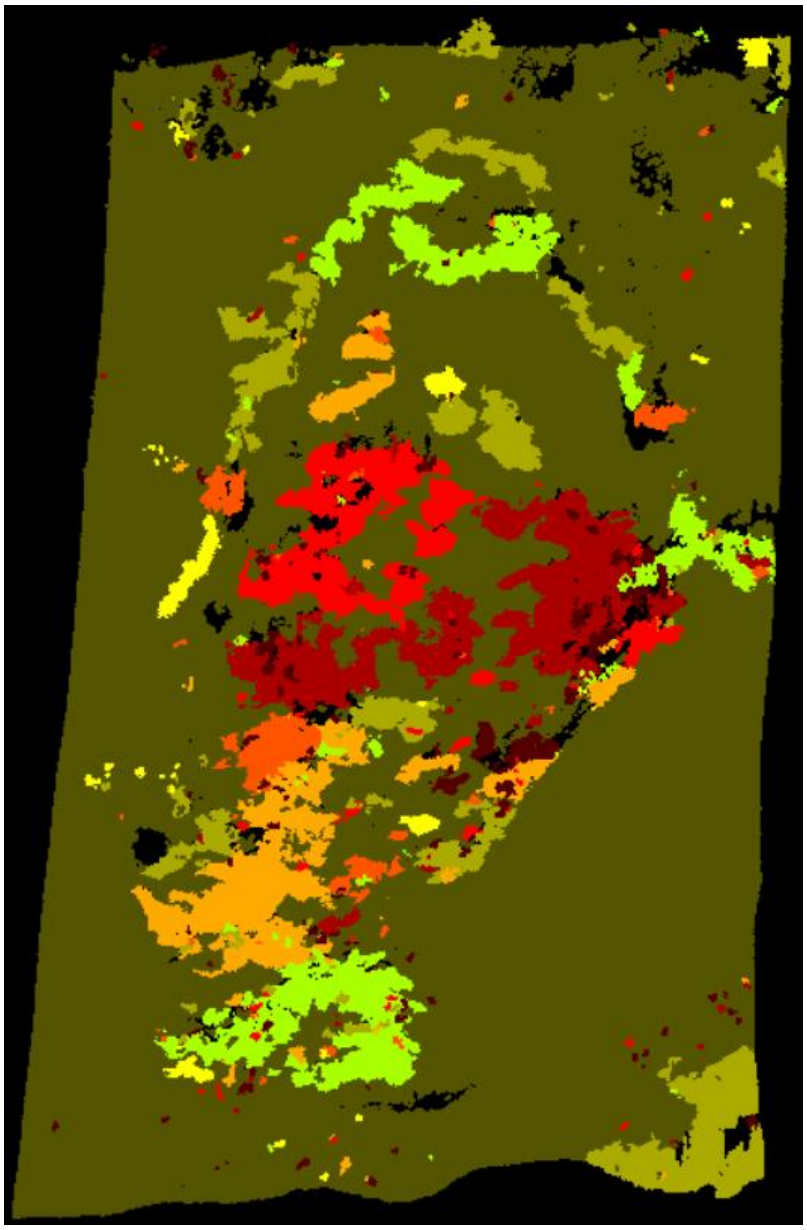

Figure 4-21: Segments coloured according to percentage of points that are dynamic between 2011 and 2013 epochs.

Figures 4-19, 4-20 and 4-21 show the amount of change per segment in each of the epochs. Generally it was observed that the segments with in the landslide and also along its boundary had a high percentage of points that were changing. However, the ground around the landslide was relatively static with few points that were changing.

4.6.3. Discussion

From the surface separation distance computed in section 4.6.1., it was seen that the dynamic parts were increasing within the landslide from 2011 to 2013. This clearly shows that something was changing or had moved. This change could be attributed to erosion especially along the boundaries of the landslide. In all epochs, a large part of the data was seen to be relatively static. The surface separation distance shows the change and the size of change per point. Grouping per segment gave a new value which showed which

segments were changing and by what amount. In all the epochs, various amounts of change were observed across the different segments with segments along and within the landslide having large amounts of change. This shows that the surface separation distance can be used as a property of objects to measure change. Although it must be noted that the quality of the change results is closely linked to the quality of the segmentation. With better segmentation results, the confidence in the change results would also increase.

4.7. Summary

In this chapter, the proposed methodology was tested using three terrestrial lidar point clouds. Before the data was used it was registered. Our registration approach improved the registration accuracy with the tilt identified in the data greatly reduced. Several point attributes that were related to the objects in the data were calculated. With the exception of the mean curvature, the rest of the point attributes were used in the different phases of the methodology. The segmentation results were fairly good; some over and under segmentation was noted though. It was also noted that for the segmentation results to be clearly interpreted, knowledge of the data/ are is crucial. This could be aided by an image of the area. Matching of the segments derived was tested but with limited success. The surface separation distance was found to show change and the amount of change taking place in each segment/ object.

5. CONCLUSIONS AND RECOMMENDATIONS

5.1. Conclusions

In this study, an object oriented approach for monitoring changes in a shallow landslide was presented. Several point attributes were calculated and used in the different phases of the study. Segmentation was then carried out followed by change detection. The conclusions of this study are split into specific conclusions for each of the research objectives as follows.

- Determining the characteristics of objects of a landslide requires knowledge of these properties. In this study, it has been shown that object properties such as slope, roughness, curvature, height above lowest local point and height difference can be derived as point attributes in a single epoch of a terrestrial lidar data. In addition, the surface separation distance was found to be useful as an object property and it was derived from multiple epochs of terrestrial lidar data. However, it important to consider the shape of the neighbourhood when computing the point attributes. This is so because some point attributes may be suited to either a 2D or 3D neighbourhood. The mean curvature and slope which are characteristic of the main scarp were not helpful in extracting the main scarp because their values were so low that using a threshold on them would introduce many false positives.
- By combining segment growing, connected components and post processing using majority filtering, segmentation results were obtained that grouped points in the point clouds to objects of a landslide. Mixed segmentation results were observed on the scarp in the different epochs. The boundary of the landslide was over segmented in all segmentation results for the different epochs. The neighbourhood size and radius were found to have no effect on the segmentation results because of the high point density of the data. However, varying the tolerance used in the segment growing showed that a large tolerance would lead to under segmentation while a low tolerance value would lead to over segmentation. An optimal tolerance value was thus used for this study.
- When matching objects/ segments between different epochs, an appropriate criterion needs to be used. In this study we tested the use of a similarity based on point attributes and minimum distance as criteria for matching. A considerable though minimal success was obtained with the later criterion. The matching of objects in the different epochs still remains a challenge because for proper matches to be obtained we need identical segments in the different epochs so that the feature values are similar. The criterion for obtaining correct matches was not completely resolved in this study. In order to measure change, the surface separation distance was presented as a way to determine change and the size of change per object/ segment. The quality of the segmentation result has a significant bearing on the quality of change results. Errors in segmentation like over or under segmentation will affect the change results. This is because this approach calculates the size of change as a percentage of the points in a segment. The volume of the object/ segment can also be used as a measure of change.
- Over and under segmentation observed in the segmentation results needs to be resolved in order to improve the quality of the segmentation. More knowledge of the object properties could help to improve the quality of the segmentation. The quality of the matching was not good. The majority of the matches between segments were incorrect. Incorporating the knowledge of how these objects move could improve this. However, the quality of the matching is highly dependent on the quality of the segmentation.

5.2. Recommendations

- Our approach is based on calculating point attributes using a local neighbourhood. It would be of interest to see whether calculating these attributes at different scales would have an effect.
- The matching criteria tested in study were based on correlation of point attributes and minimum distance between segments. It would be of interest to test if using different matching criteria for objects that are static and dynamic would have an effect.

LIST OF REFERENCES

Abellán, A., Oppikofer, T., Jaboyedoff, M., Rosser, N. J., Lim, M., & Lato, M. J. (2014). Terrestrial laser scanning of rock slope instabilities. *Earth Surface Processes and Landforms*, *39*(1), 80–97. doi:10.1002/esp.3493

Anders, N. S., Seijmonsbergen, A. C., & Bouten, W. (2013). Geomorphological Change Detection Using Object-Based Feature Extraction From Multi-Temporal LiDAR Data. *IEEE Geoscience and Remote Sensing Letters*, *10*(6), 1587–1591. doi:10.1109/LGRS.2013.2262317

Center for Research on the Epidemilogy of Disasters. (2012). Annual Disaster Statistical Review. Retrieved from http://www.cred.be/sites/default/files/ADSR_2012.pdf

Chigira, M., Duan, F., Yagi, H., & Furuya, T. (2004). Using an airborne laser scanner for the identification of shallow landslides and susceptibility assessment in an area of ignimbrite overlain by permeable pyroclastics. *Landslides*. Retrieved from http://link.springer.com/article/10.1007/s10346-004-0029-x

Choi, K., Lee, I., & Kim, S. (2009). A feature based approach to automatic change detection from Lidar Data in urban areas. *International Archives of Photogrammetry, Remote Sensing and Spatial Information Sciences*, 259–264.

Chung, J., Rogers, J. D., & Watkins, C. M. (2014). Estimating severity of seismically induced landslides and lateral spreads using threshold water levels. *Geomorphology*, *204*, 31–41. doi:10.1016/j.geomorph.2013.07.024

Cruden, D. M., & Varnes, D. J. (1996). Landslides: Investigation and Mitigation. Chapter 3-Landslide types and processes. *Transportation Research Board Special Report*, (247).

Deng, S., & Shi, W. (2014). Semi-automatic approach for identifying locations of shallow debris slides/flows based on lidar-derived morphological features. *International Journal of Remote Sensing*, *35*(10), 3741–3763. doi:10.1080/01431161.2014.915438

Dewitte, O., Jasselette, J.-C., Cornet, Y., Van Den Eeckhaut, M., Collignon, A., Poesen, J., & Demoulin, A. (2008). Tracking landslide displacements by multi-temporal DTMs: A combined aerial stereophotogrammetric and LIDAR approach in western Belgium. *Engineering Geology*, *99*(1-2), 11–22. doi:10.1016/j.enggeo.2008.02.006

Glenn, N. F., Streutker, D. R., Chadwick, D. J., Thackray, G. D., & Dorsch, S. J. (2006). Analysis of LiDAR-derived topographic information for characterizing and differentiating landslide morphology and activity. *Geomorphology*, *73*(1-2), 131–148. doi:10.1016/j.geomorph.2005.07.006

Goudie, A. (2004). *Encyclopedia of geomorphology* (Vol. 2). Psychology Press.

Gutiérrez, F., Soldati, M., Audemard, F., & Bălteanu, D. (2010). Recent advances in landslide investigation: Issues and perspectives. *Geomorphology*, *124*(3-4), 95–101. doi:10.1016/j.geomorph.2010.10.020

Hervás, J., Barredo, J. I., Rosin, P. L., Pasuto, A., Mantovani, F., & Silvano, S. (2003). Monitoring landslides from optical remotely sensed imagery: the case history of Tessina landslide, Italy. *Geomorphology*, *54*(1-2), 63–75. doi:10.1016/S0169-555X(03)00056-4

Jaboyedoff, M., Oppikofer, T., Abellán, A., Derron, M.-H., Loye, A., Metzger, R., & Pedrazzini, A. (2010). Use of LIDAR in landslide investigations: a review. *Natural Hazards*, *61*(1), 5–28. doi:10.1007/s11069-010-9634-2

Lu, P., Stumpf, A., Kerle, N., & Casagli, N. (2011). Object-Oriented Change Detection for Landslide Rapid Mapping. *IEEE Geoscience and Remote Sensing Letters*, *8*(4), 701–705. doi:10.1109/LGRS.2010.2101045

Martha, T. R., Kerle, N., Jetten, V., van Westen, C. J., & Kumar, K. V. (2010). Characterising spectral, spatial and morphometric properties of landslides for semi-automatic detection using object-oriented methods. *Geomorphology*, *116*(1-2), 24–36. doi:10.1016/j.geomorph.2009.10.004

McKean, J., & Roering, J. (2004). Objective landslide detection and surface morphology mapping using high-resolution airborne laser altimetry. *Geomorphology*, *57*(3-4), 331–351. doi:10.1016/S0169-555X(03)00164-8

Metternicht, G., Hurni, L., & Gogu, R. (2005). Remote sensing of landslides: An analysis of the potential contribution to geo-spatial systems for hazard assessment in mountainous environments. *Remote Sensing of Environment*, *98*(2-3), 284–303. doi:10.1016/j.rse.2005.08.004

Murakami, H., Nakagawa, K., Hasegawa, H., Shibata, T., & Iwanami, E. (1999). Change detection of buildings using an airborne laser scanner. *ISPRS Journal of Photogrammetry and Remote Sensing*, *54*(2-3), 148–152. doi:10.1016/S0924-2716(99)00006-4

Pesci, A., Teza, G., Casula, G., Loddo, F., De Martino, P., Dolce, M., … Pingue, F. (2011). Multitemporal laser scanner-based observation of the Mt. Vesuvius crater: Characterization of overall geometry and recognition of landslide events. *ISPRS Journal of Photogrammetry and Remote Sensing*, *66*(3), 327–336. doi:10.1016/j.isprsjprs.2010.12.002

Qiao, G., Lu, P., Scaioni, M., Xu, S., Tong, X., Feng, T., … Li, R. (2013). Landslide Investigation with Remote Sensing and Sensor Network: From Susceptibility Mapping and Scaled-down Simulation towards in situ Sensor Network Design. *Remote Sensing*, *5*(9), 4319–4346. doi:10.3390/rs5094319

Razak, K. A., Straatsma, M. W., van Westen, C. J., Malet, J.-P., & de Jong, S. M. (2011). Airborne laser scanning of forested landslides characterization: Terrain model quality and visualization. *Geomorphology*, *126*(1-2), 186–200. doi:10.1016/j.geomorph.2010.11.003

Regmi, N. R., Giardino, J. R., & Vitek, J. D. (2013). Characteristics of landslides in western Colorado, USA. *Landslides*, *11*(4), 589–603. doi:10.1007/s10346-013-0412-6

Roessner, S., Behling, R., Segl, K., Golovko, D., Wetzel, H.-U., & Kaufmann, H. (2014). Automated Remote Sensing Based Landslide Detection for Dynamic Landslide Inventories. In K. Sassa, P. Canuti, & Y. Yin (Eds.), *Landslide Science for a Safer Geoenvironment* (pp. 345–350). Cham: Springer International Publishing. doi:10.1007/978-3-319-05050-8

Rottensteiner, F. (2010). Automation of object extraction from LiDAR in urban areas. doi:10.1109/IGARSS.2010.5652949

Stumpf, A., Malet, J.-P., Allemand, P., Pierrot-deseilligny, M., & Skupinski, G. (2015). Geomorphology Ground-based multi-view photogrammetry for the monitoring of landslide deformation and erosion. *Geomorphology*, *231*, 130–145. doi:10.1016/j.geomorph.2014.10.039

Tarolli, P., Sofia, G., & Dalla Fontana, G. (2010). Geomorphic features extraction from high-resolution topography: landslide crowns and bank erosion. *Natural Hazards*, *61*(1), 65–83. doi:10.1007/s11069-010-9695-2

Teo, T.-A., & Shih, T.-Y. (2013). Lidar-based change detection and change-type determination in urban areas. *International Journal of Remote Sensing*, *34*(3), 968–981. doi:10.1080/01431161.2012.714504

Travelletti, J., Malet, J.-P., & Delacourt, C. (2014). Image-based correlation of Laser Scanning point cloud time series for landslide monitoring. *International Journal of Applied Earth Observation and Geoinformation*, *32*, 1–18. doi:10.1016/j.jag.2014.03.022

Van Den Eeckhaut, M., Kerle, N., Poesen, J., & Hervás, J. (2012). Object-oriented identification of forested landslides with derivatives of single pulse LiDAR data. *Geomorphology*, *173-174*, 30–42. doi:10.1016/j.geomorph.2012.05.024

Ventura, G., Vilardo, G., Terranova, C., & Sessa, E. B. (2011). Tracking and evolution of complex active landslides by multi-temporal airborne LiDAR data: The Montaguto landslide (Southern Italy). *Remote Sensing of Environment*, *115*(12), 3237–3248. doi:10.1016/j.rse.2011.07.007

Vögtle, T., & Steinle, E. (2004). Detection and recognition of changes in building geometry derived from multi-temporal laser scanning data. *International Archives of the Photogrammetry, Remote Sensing and Spatial Information Sciences*, *34*, 428–433.

Vosselman, G. (2013). Point cloud segmentation for urban scene classification. *ISPRS-International Archives of* …. Retrieved from http://www.int-arch-photogramm-remote-sens-spatial-inf-sci.net/XL-7-W2/257/2013/isprsarchives-XL-7-W2-257-2013.pdf

Wang, G., Joyce, J., Phillips, D., Shrestha, R., & Carter, W. (2013). Delineating and defining the boundaries of an active landslide in the rainforest of Puerto Rico using a combination of airborne and terrestrial LIDAR data. *Landslides*, *10*(4), 503–513. doi:10.1007/s10346-013-0400-x

Wiegand, C., Kringer, K., Geitner, C., & Rutzinger, M. (2013). Regolith structure analysis — A contribution to understanding the local occurrence of shallow landslides (Austrian Tyrol). *Geomorphology*, *183*, 5–13. doi:10.1016/j.geomorph.2012.06.027

Xiao, W., Xu, S., Oude Elberink, S., & Vosselman, G. (2012). Change detection of trees in urban areas using multi-temporal airborne lidar point clouds. In C. R. Bostater, S. P. Mertikas, X. Neyt, C. Nichol, D. Cowley, & J.-P. Bruyant (Eds.), *SPIE Remote Sensing* (p. 853207). International Society for Optics and Photonics. doi:10.1117/12.974266

Xu, S., Vosselman, G., & Oude Elberink, S. (2013). Detection and classification of changes in buildings from airborne laser scanning data. *ISPRS Annals of Photogrammetry, Remote Sensing and Spatial Information Sciences*, *II-5/W2*(November), 343–348. doi:10.5194/isprsannals-II-5-W2-343-2013

Appendix 1: Tree segments